STRUCTURE AND CATALYTIC ACTIVITY OF $NiO-Al_2O_3$ SYSTEMS

A Thesis Submitted
In Partial Fulfilment of the Requirements
For the Degree of
DOCTOR OF PHILOSOPHY

by

RAMANATHAN ATHAPPAN

to the

DEPARTMENT OF CHEMICAL ENGINEERING
INDIAN INSTITUTE OF TECHNOLOGY, KANPUR

FEB, 1979

TO

MY PARENTS

CERTIFICATE

This is to certify that the work 'STRUCTURE AND CATALYTIC ACTIVITY OF NiO-Al_2O_3 SYSTEMS' has been carried out under my supervision and that this has not been submitted elsewhere for a degree.

Date: February 9 ,1979

R D Srivastava

[R.D. SRIVASTAVA]
Professor and Head
Department of Chemical Engineering
Indian Institute of Technology
Kanpur-208016,India

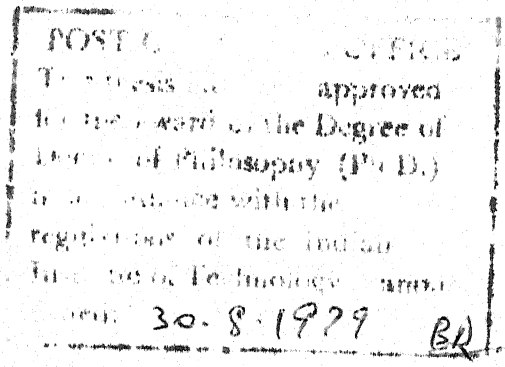

ACKNOWLEDGEMENTS

The author expresses his grateful thanks to Professor R.D. Srivastava who spared no pains in giving inspiring guidance, valuable advice, and meticulous attention in each and every step of this investigation.

To Dr. K.N. Rai of Materials Science, Indian Institute of Technology, Kanpur for his helpful assistance and guidance in the interpretation of Electron Micrographs.

To Dr. Anil Kumar for providing Chromatographic facilities.

To the helpful cooperation offered by the fellow student friends and departmental staff from time to time.

Special appreciation is extended to Mr. B.S. Pandey for the great care he bestowed in typing the manuscript and to Mr. D.S. Panesar for tracing the figures.

To Dr.(Mrs.) Indira Athappan for her helpful assistance in writing this manuscript.

Author

CONTENTS

SYNOPSIS

The thesis consists of four major sections. Section 1 deals with the solid state properties of $NiO-Al_2O_3$ systems. Section 2 is devoted to the catalytic activity of $NiO-Al_2O_3$ systems for the vapour phase decomposition of cyclohexanol. Kinetics and mechanisms for the parallel dehydrogenation and dehydration of cyclohexanol over $NiO-Al_2O_3$ systems are given in section 3. Section 4 deals with the liquid phase oxidation of tetralin over $NiO-Al_2O_3$ systems.

Supported $NiO-Al_2O_3$ catalysts containing upto 20 per cent by weight of NiO calcined at 450°C for 12 hours have been studied by means of various chemico-physical techniques. The internal distribution of the active species, size and shape has been determined using electron microscopy. The thermal analyses indicate that at 400°C, NiO is formed which remains unchanged on further heating. Evidence for the spinel formation nickel-aluminate was not indicated by X-ray and electron microscopy.

The catalytic vapour phase decomposition of cyclohexanol has been studied over NiO supported on Al_2O_3. Experiments have been carried out to study the influence of content of active phase in the catalyst and reaction temperature on catalytic activity. Catalyst containing 20 per cent by weight of NiO (NiO-20-450-12) exhibits a less activity which is shown to be related to the crystal growth of nickel oxide on the

support Al_2O_3. The product distribution strongly suggested two distinct regions in the activity of $NiO-Al_2O_3$ systems; parallel dehydrogenation and dehydration in the low temperature region (300-350°C); consecutive dehydration and dehydrogenation in the high temperature region (350-400°C).

Kinetics of parallel dehydrogenation and dehydration of cyclohexanol on $NiO-Al_2O_3$ system have been investigated in an isothermal packed bed reactor at atmospheric pressure between 300-350°C. Various Hougen and Watson types of rate equations were examined by linear and nonlinear estimations. The later treatment showed the adsorption of water reduced the dehydration rate and must be included in any mechanism. A statistically best rate expression was obtained for both dehydrogenation and dehydration reactions from the experimental data.

Kinetics of liquid phase oxidation of tetralin was investigated between the temperatures of 45-85°C at regular intervals of 10°C with $NiO-Al_2O_3$ systems. The effects of catalyst ratio, catalyst composition, catalyst calcination period and hydrocarbon concentration on the reaction rate were studied. A rate expression was derived from the proposed mechanism.

SECTION 1

SOLID STATE PROPERTIES OF $NiO-Al_2O_3$ SYSTEMS

CONTENTS

LIST OF FIGURES

LIST OF TABLES

NOMENCLATURE

a, b, c	Lattice parameters, $\mathring{A}$
d	Distance between each set of atomic planes of crystal lattice

Greek Symbols

θ	Angle of diffraction
α, β, γ, k	Different phases of alumina

1.1 INTRODUCTION

In the past 25 years, supported metal oxide systems have been one of the major areas of investigation in heterogeneous catalysis. These systems find wide applications in many important industrial processes such as oxidation, reduction, hydrogenation and dehydrogenation. Supported NiO provides an example for the various problems encountered when dealing with an active component NiO dispersed over an inert support (Al_2O_3).

A number of authors [1-8] have treated the thermal, structural, mechanical and electrical properties of alumina-supported nickel oxide in the temperature range of 600-1500°C in some detail, however, very little is reported of the characterization of nickel oxide-alumina catalyst in the temperature below 600°C [9-11]. Some of these authors [10-11] have X-ray evidence for spinel formation at 600°C or below, however, others [9] failed to have direct identification for spinel formation.

Kurkova et al. [1] studied the effect of active components NiO, Fe_2O_3 CoO, MnO_2 Cr_2O_3 and V_2O_5 on the rate of phase transformations in γ-Al_2O_3 in Al_2O_3 supported catalyst systems. For the Al_2O_3-NiO catalyst containing 10 per cent NiO appeared some what more stable than Al_2O_3. This may be associated with the formation of a solid solution of the spinel $NiAl_2O_4$ in the Al_2O_3.

Gavrish and Zoz [2] investigated the change in the phase composition of carrier while heating in oxidizing and reducing media. The changes in the properties and phase composition were established with increasing concentration of nickel nitrate hexahydrate. Weak traces of $NiAl_2O_4$ were observed after holding the samples at 900°C. The formation of $NiAl_2O_4$ is practically completed at 1300°C.

The influence of carriers on the physico-chemical properties of NiO were reported by Umemura [3]. Domaka et al. [4] investigated the influence of the temperature of calcination of Ni, Fe oxide catalysts on some of their physico-chemical and catalytic properties. The catalytic test reaction was the decomposition of isopropyl alcohol and the cracking of cumene. The phase boundary surfaces of the $NiO-Fe_2O_3-NiFe_2O_4$ system to be the main source of the catalytic activity of these oxides.

Katsobashvilt et al. [5] studied the effect of chemical composition of Al_2O_3 impregnated with NiO, MoO_3 and Cr_2O_3 catalysts on the stability of their structural and mechanical properties during heat treatment. NiO increased the structura and mechanical properties of the heated catalyst and Cr_2O_3 was of no significant effect.

Jaconu et al. [6] employed X-ray analysis, reflectance spectroscopy and magnetic measurements to investigate the interaction which takes place when nickel oxide is supported

on η and γ-Al_2O_3. It was found that a 'surface spinel' $NiAl_2O_4$ is formed.

There appears to be no prior detailed study on the solid state properties of supported NiO-Al_2O_3 catalyst systems. In order to contribute to the literature and to clear up some aspects concerning the nature of the active sites in relation to the catalytic activity, investigations have been carried out with a series of supported NiO-Al_2O_3 catalysts.

This section aims to elucidate the solid state properties of NiO-Al_2O_3 systems. Supported NiO-Al_2O_3 catalyst systems containing upto 20 weight per cent NiO have been studied in detail by means of electron microscopy, DTA, TGA, DTG, X-ray, IR and B.E.T. studies.

1.2 EXPERIMENTAL

1.2.1 Preparation of Catalyst

The experimental system studied was the impregnation of gamma alumina with nickel nitrate hexahydrate. Gamma alumina supported catalysts containing 5 to 20 per cent by weight of NiO were prepared by the method of impregnation recommended for the mixed catalysts [12-14]. Reference to various samples will be made by giving their composition as weight per cent of NiO followed by temperature and duration of calcination; hence NiO-5-450-12 means a sample of NiO supported on alumina having 5 per cent of the active element as NiO heat treated at 450°C for 12 hours in air.

1.2.2 Physico-Chemical Characterization

(a) X-ray powder analysis

X-ray powder diffraction spectra were obtained at room temperature using General Electronic Diffractometer (XRD-VI-Generator SPG-4 detector and SPG-2 Diffractometer) with nickel filtered Cu(Kα) radiation. The diffractometer was operated with 2° diverging and receiving slits at a scan rate of 1° per minute and a continuous trace of intensity as a function of 2 θ were recorded. Spectra of finely ground samples were run in the 2 θ range of 0 - 70°.

(b) Infrared spectroscopy

Transmittance spectra of powdered samples ($\lesssim$ 200 mesh) were recorded in the range of 4000-250 cm^{-1} on a Perkin-Elmer -521 Grating infrared spectrophotometer using KBr disc.

(c) DT and TG analysis

Differential thermal analysis and thermogravimetric analysis of the samples were carried out simultaneously using a complex thermo analytical equipment [Derivalograph, M.O.M. Budapest]. As a reference material α-Al_2O_3 was used. All the experiments were conducted in air at atmospheric pressure at a heating rate of $10^{o}C\ min^{-1}$. In the TGA experiments 650 mg of the samples were heated at the same heating rate until a constant weight was obtained.

(d) Surface area and pore volume

Surface area of the catalysts were determined from N_2 adsorption isotherms using B.E.T. apparatus. Pore volume and pore size distribution were measured by a mercury porosimeter.

(e) Electron microscopy:

The transmission electronmicroscopy was carried out mainly to study the interaction of NiO with gamma alumina and also to estimate the particle size distribution of pure gamma Al_2O_3 and alumina supported NiO catalysts. Specimen

preparations were accomplished by suspending the particle of gamma alumina, nickel oxide and supported nickel oxide catalysts in 1 per cent collodion solution with the help of ultrasonic vibrator. The collodion plastic films were prepared by adding a drop of the above suspension over distilled water. The film was then finally mounted over 200 mesh copper support grid of 3 mm diameter. Particles of alumina and supported catalysts get embedded in the collodion film which provides better stability during electron microscopy.

The Philips E.M. 301 electron microscope excited at 80 KV with eugocentic goniometer at a resolution better than 10 Å was used during this investigation. The magnification and rotation calibrations were carried out by standard procedures. The diffraction camera constant (λL) was calibrated for 80 KV at a particular lense setting using (111), (200), (220) and (311) diffraction lines from evaporated pure gold film.

1.3 RESULTS AND DISCUSSION

1.3.1 X-ray:

X-ray powder spectra reveal the presence of both components NiO and Al_2O_3 in all the samples examined. The d values for the NiO and γ-Al_2O_3 are given in Tables 1 and 2, calculated from the X-ray powder diffraction patterns. The d values are in excellent agreement with the d values reported for NiO and γ-Al_2O_3 [15, 22]. The results of the analyses of the separate samples are given in Figure 1. There is an indication that the intensity of the line at the corresponding 2θ values 37.4° (d = 2.41 Å), 43.4°(d = 2.08Å) and 62.8° (d = 1.476 Å) increases with increased amount of NiO in the specimen. If attention is focussed on the intensity of the lines of pure alumina and nickel containing specimens as compared to those of $NiAl_2O_4$ [6], the absence of the diffractic line corresponding to the 2θ value of 19.8° (d = 4.5 Å) indicated a lack in the formation of $NiAl_2O_4$ under the conditions of the system studied. This has also been noted by some authors [16, 17] previously. Although the evidence for the presence of $NiAl_2O_4$ on the surface of alumina is not easily offered by the X-ray techniques alone, electron microscopy has further supported the absence of spinel formation. The results of electron microscopic studies are described later in the text.

TABLE 1: d-VALUES FOR NiO

ASTM 4-0835 [15] d-Values Å	Calculated d-Values Å
2.4100	2.4088
2.0880	2.0880
1.4760	1.4750
1.2590	1.2600
1.2060	1.2060
1.0440	1.0430
0.9582	-
0.9338	-
0.8527	-

TABLE 2: d-VALUES FOR γ-Al_2O_3

ASTM 10-425 [15] d Values Å	Calculated d Values Å
4.560	4.530
2.800	2.784
2.390	2.387
2.280	2.278
1.977	1.970
1.520	-
1.395	1.398
1.140	-
1.027	-
0.989	-
0.884	-

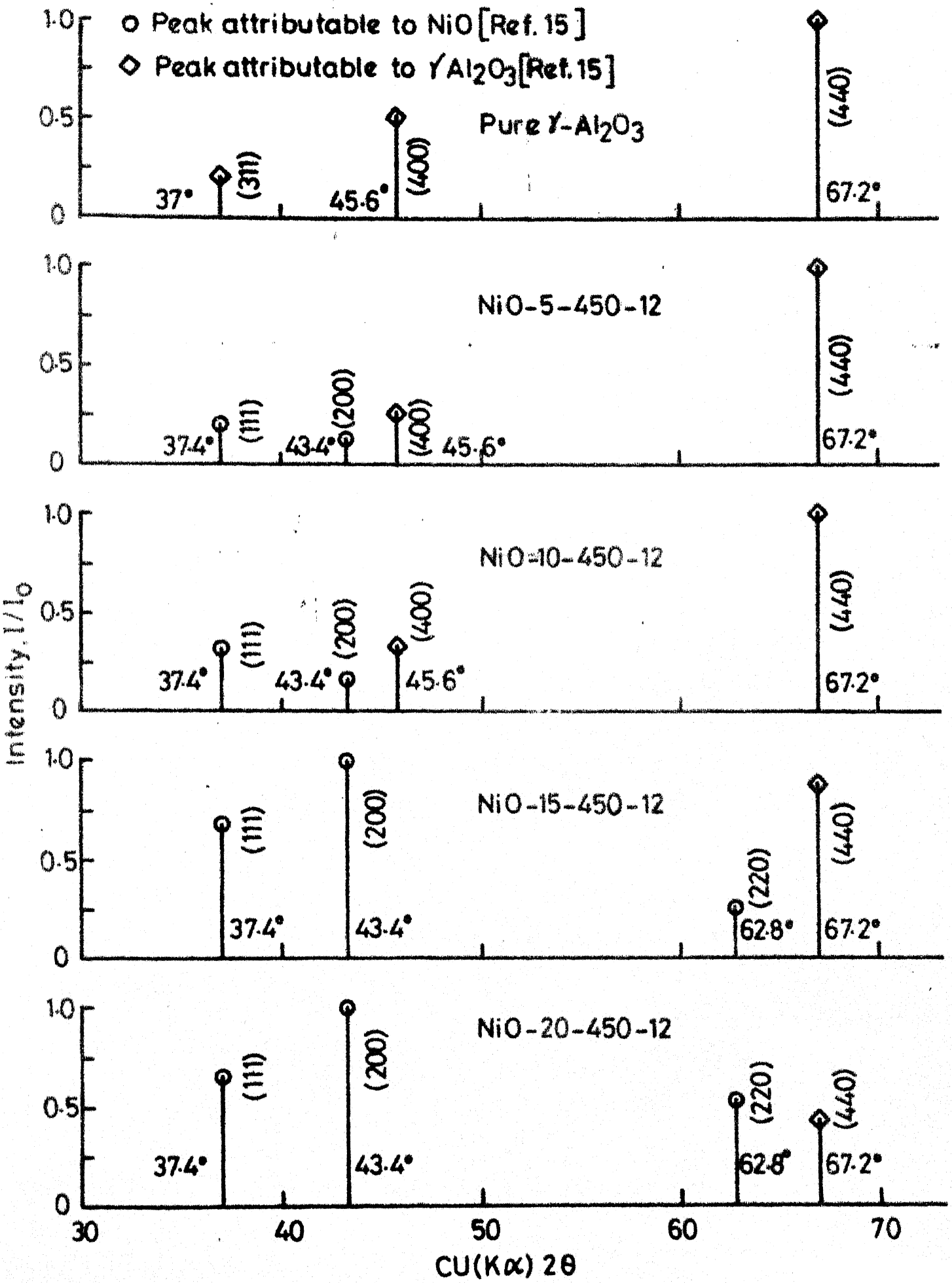

Fig. 1 - X-ray diffractograms.

1.3.2 Infrared Spectroscopy

In the transmittance spectra of NiO-Al_2O_3 systems (0-20 weight per cent NiO calcined in air at 450°C for 12 hours); we noticed intense absorption of NiO (Plateau in the 800-400 cm^{-1} region) covering any diagnostic Al-O frequency in the bulk. The 900 cm^{-1} Al-O (plateau in the 940-500 cm^{-1} region) resolved into set of components at 925 and 885 cm^{-1} which is attributable to free Al_2O_3 present in the bulk. The transmittance spectra of Al_2O_3 and NiO were similar to previously reported spectra of these oxides [18, 19].

1.3.3 DT and TG Analysis:

The DTA thermograms for the catalysts are shown in Figure 2. The DTA analyses of all catalyst samples calcined at 450° for 12 hours show an endo-thermal transformation at 110°C. Except the 5 per cent NiO on Al_2O_3 sample, others show no further transformation till 600°C. In the case of 5 per cent NiO catalyst sample a small endothermal drift was observed at 300°C. These endothermic transformations are may be due to the atmospheric and crystalline water of dehydration.. In all the catalysts a small endothermal transformation was observed around 700°C which may be due to the phase transformation of γ-Al_2O_3 to α-Al_2O_3.

The color of all the catalyst samples prior to DT analysis varied from green, greyish green to black as the

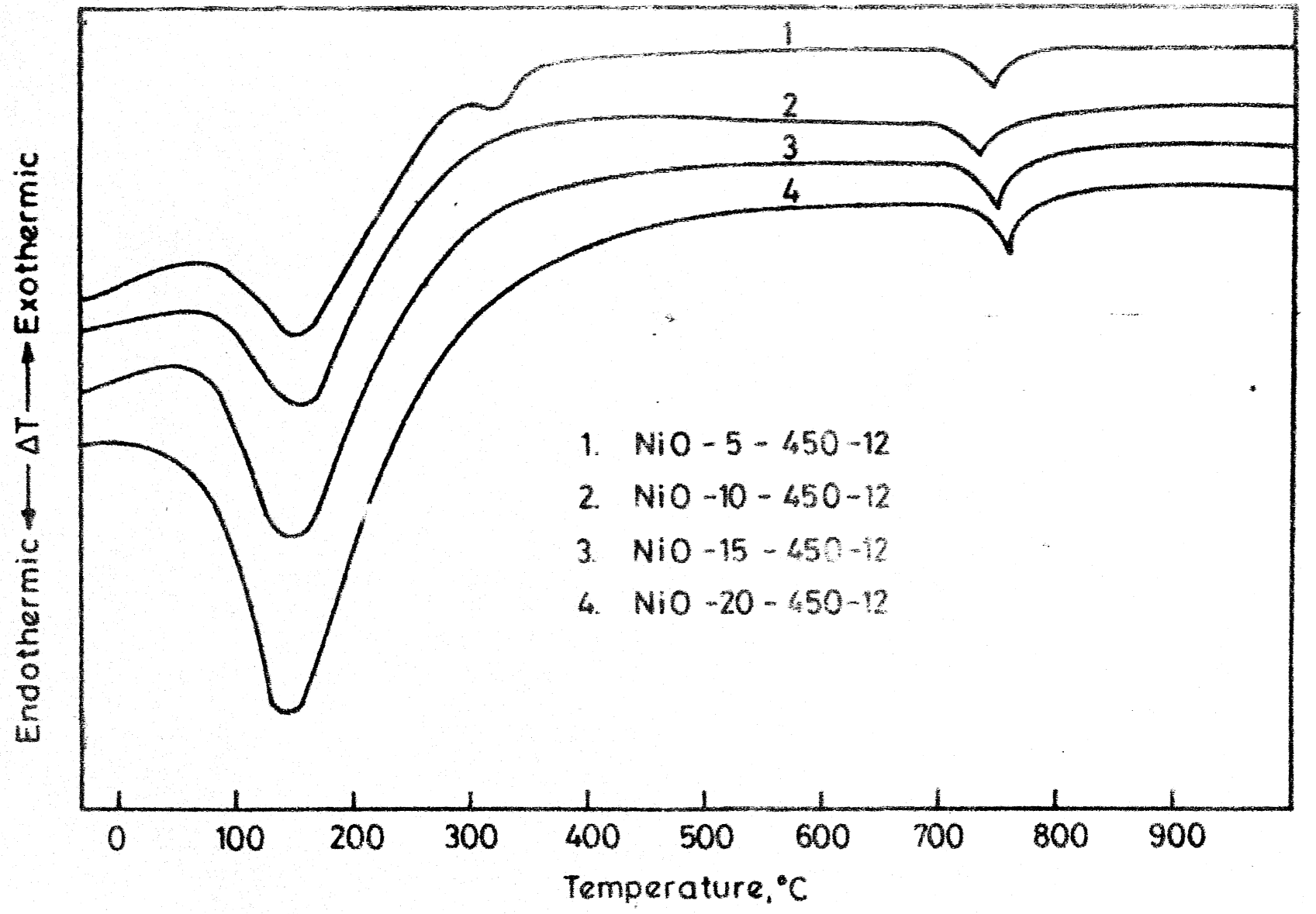

Fig 2 - Differential thermal analysis thermograms.

weight per cent of the active component NiO increases in the catalyst samples. At the end of the DT analysis, we observed the color of all the catalyst samples changed to blue color which could be accounted for the gamma to alpha phase transformation of alumina [6].

TG analysis was performed with programmed temperature increase at a rate of 10°C per minute. The weight loss (in mg) as a function of temperature for all the samples are illustrated in Figure 3. From the TG analysis it has been observed that there is a gradual loss in weight which is mainly due to the release of excess oxygen that NiO contained when prepared by low temperature decomposition of nickel nitrate hexahydrate. The presence of excess oxygen in the catalyst samples are indicated by the gradual increase of the black color of the samples. These observations are similar to those reported previously [20, 21].

TG analysis was also performed for the pure nickel nitrate hexahydrate which was used in the catalyst preparations. The decomposition of the nickel nitrate hexahydrate to nickeloxide in air is complete at 400°C as indicated by the observed weight loss of 75 per cent compared with the calculated value of 74.3 per cent for the conversion of nickel nitrate hexahydrate to nickeloxide.

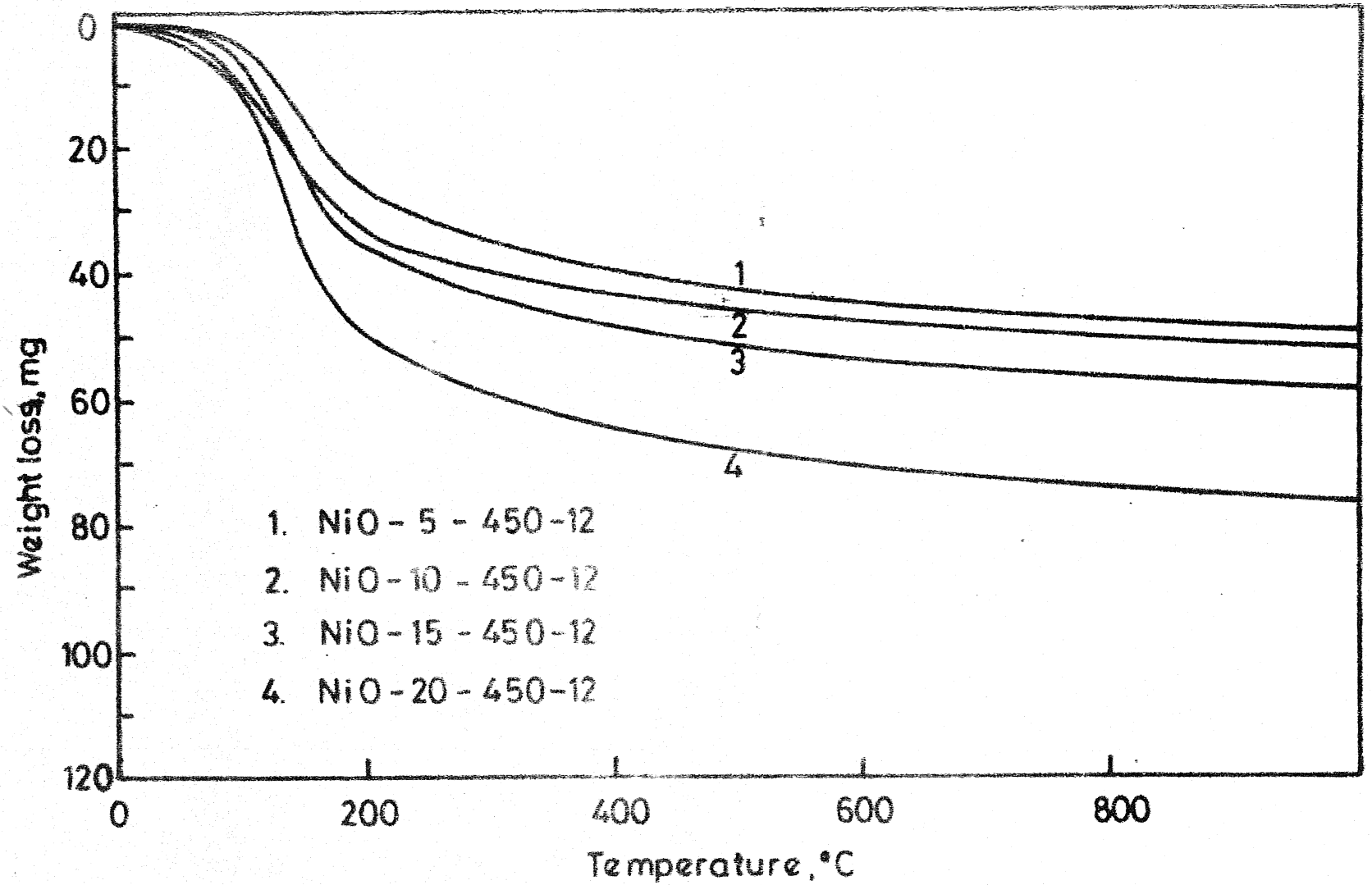

Fig. 3 - Thermogravimetric analysis.

1.3.4 Surface Area and Pore Volume

Surface area (S_A), pore volume (V_P) and porosity of the samples together with the calculated value of pore radii [$\bar{r} = 2\ V_P/S_A$] are given in Table 3.

1.3.5 Microstructure and Crystal Structure of γ-Alumina

Electron microscopic observations show that the alumina particles have interconnected pores forming channels of about 50 Å diameter. Though major portion of the alumina powder used in our study contains gamma alumina, close examination by the electron diffraction shows the existence of other forms of alumina. Figure 4 shows an alumina grain containing parallel micro-twin bands. The corresponding electron diffraction is given in Figure 4 b. The d values calculated from this for several spots correspond to κ-alumina (a = 9.71 Å, C = 17.86 Å hexagonal system), however, the complete indexing seems to be impossible. It is also interesting to note from electron diffraction that the grain structure has the tendency of displaying streaks due to one dimensional disorder and probably super lattice reflections. Similarly other forms of alumina seem to coexist with the gamma alumina which cannot be deducted by the X-ray diffraction methods because of their bulk proportions being too small. Apart from this some grain appears to be very sensitive to electron beam. They tend to recrystallize with high exposure as evidenced from Figure 4c.

TABLE 3: SURFACE AREA, PORE VOLUME AND AVERAGE PORE RADIUS

Catalyst	S_A m^2/g	V_P cc/g	Porosity cc/100 cc	$\bar{r} = \frac{2V_P}{S_A}$ in Å	Pore Size Distribution, Å						
					4-60	60-100	100-200	200-300	300-400	400-500	500-7500
NiO-5-450-12	96	0.3178	53.1	66.20	40.7	9.8	7.7	4.7	2.5	2.2	32.4
NiO-10-450-12	97.5	0.2994	52.0	61.41	39.7	9.1	8.0	3.8	2.9	2.1	34.4
NiO-15-450-12	87.6	0.2753	50.7	62.80	46.0	6.3	5.4	2.9	1.9	1.3	36.2
NiO-20-450-12	77.9	0.2739	51.6	70.32	52.0	4.9	4.0	2.6	1.9	1.4	33.2
Al_2O_3	103.3	0.3311	55.1	64.27	56.5	14.5	8.9	3.9	0.4	0.9	12.6

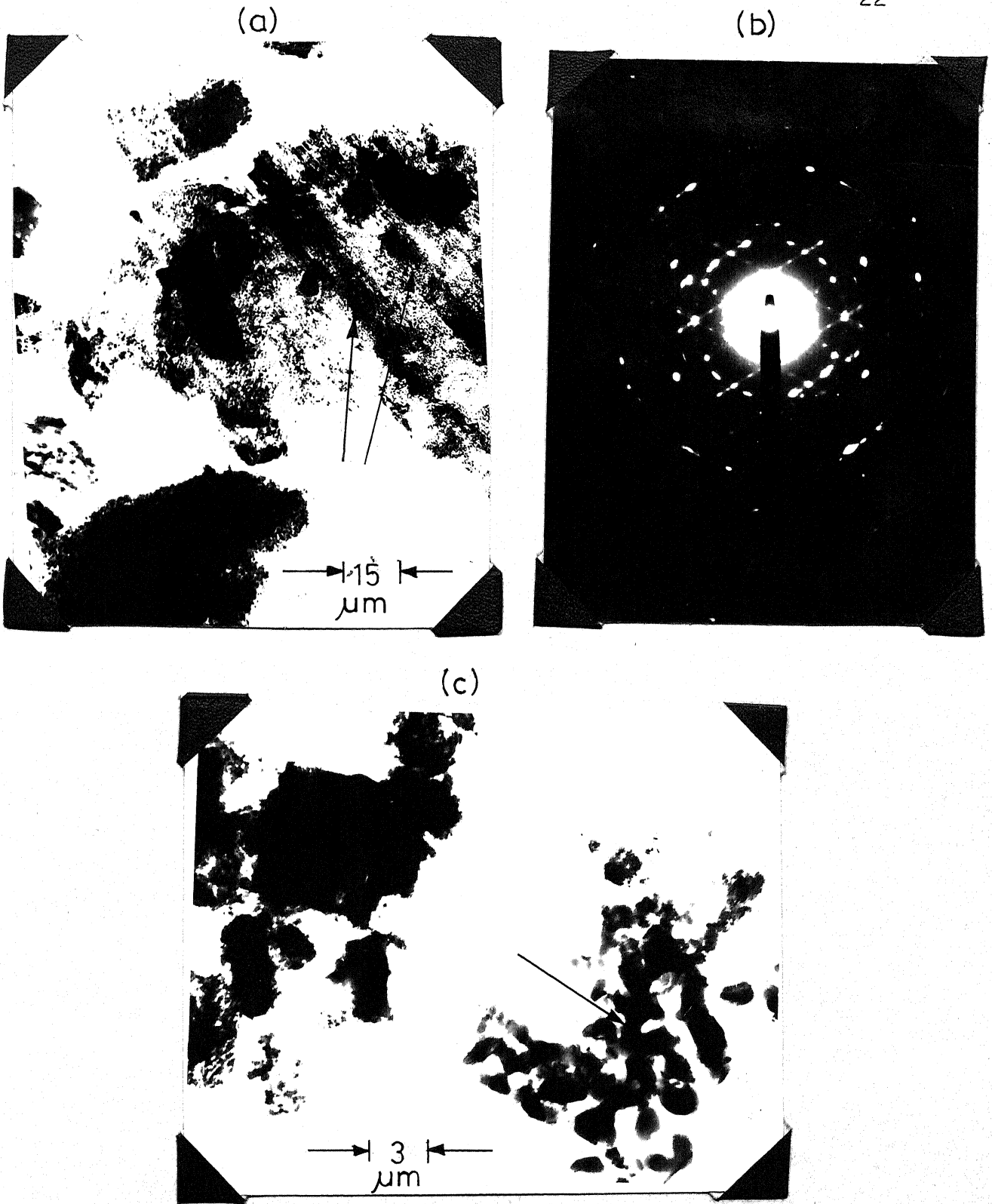

FIGURE 4: ELECTRON MICROGRAPH OF PURE γ-Al_2O_3 GRAINS

(a) Pure γ-Al_2O_3 Grain

(b) Diffraction of (a) Pure γ-Al_2O_3 Grain

(c) Micrograph Showing Recrystallization of Pure γ-Al_2O_3 Grain

1.3.6 Electron Microscopy of $NiO-Al_2O_3$ Supported Materials:

Figures5a, b, c and d show the electron micrographs of alumina grains impregnated with 5 per cent, 10 per cent, 15 per cent and 20 per cent NiO. The thin area of micrograph of Figure 5a. indicates particles of NiO of about 55 Å dispersed homogeneously. As the concentration of catalyst increases the crowding of particles increases. Thus it is difficult to resolve isolated NiO particles at higher concentrations. In fact NiO appears to form continuous thick layer throughout the surface.

The electron diffraction patterns for the 15 per cent and 20 per cent NiO catalysts are shown in Figures 6a and b. The continuous lines can be indexed in terms of pure NiO (f.c.c. structure a = 4.177 Å) and the residual electron diffraction spots can be indexed on the basis of gamma and other forms of alumina. We did not find any evidence to support the existence of nickel aluminate. It clearly shows that atleast NiO is not structurally affected by Al_2O_3. The hexagonal spot pattern visible in Figure 6a. for 15 per cent NiO seems to be indexable on the basis of Chi-Al_2O_3 (a = 5.56 Å and c = 13.44 Å). However, it does not mean that the structure has resulted due to NiO. In fact the study of pure alumina reveals that in addition to γ-Al_2O_3 several structures exist within a small alumina particle.

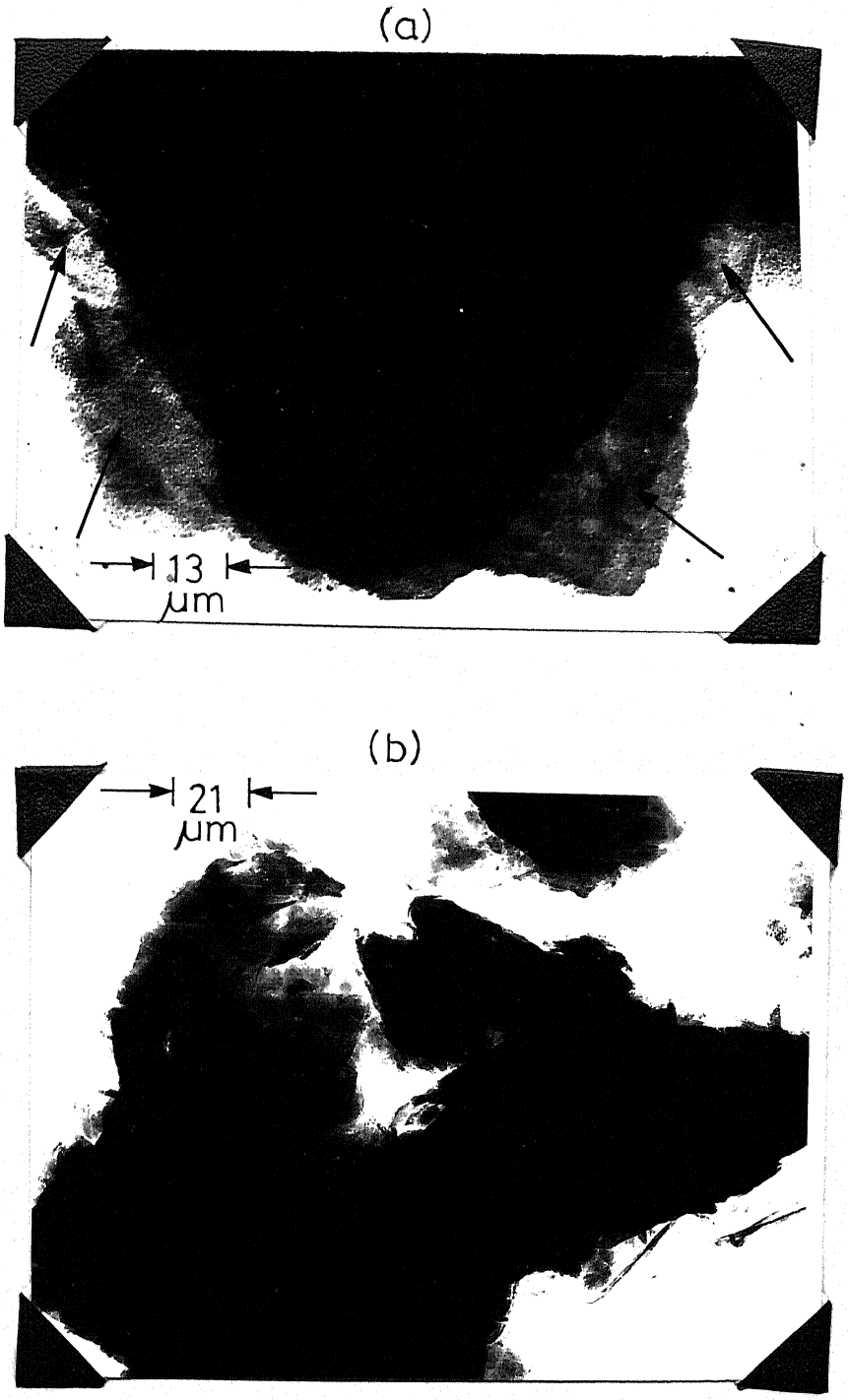

FIGURE 5: ELECTRON MICROGRAPH OF SINGLE GRAINS
(a) NiO-5-450-12
(b) NiO-10-450-12

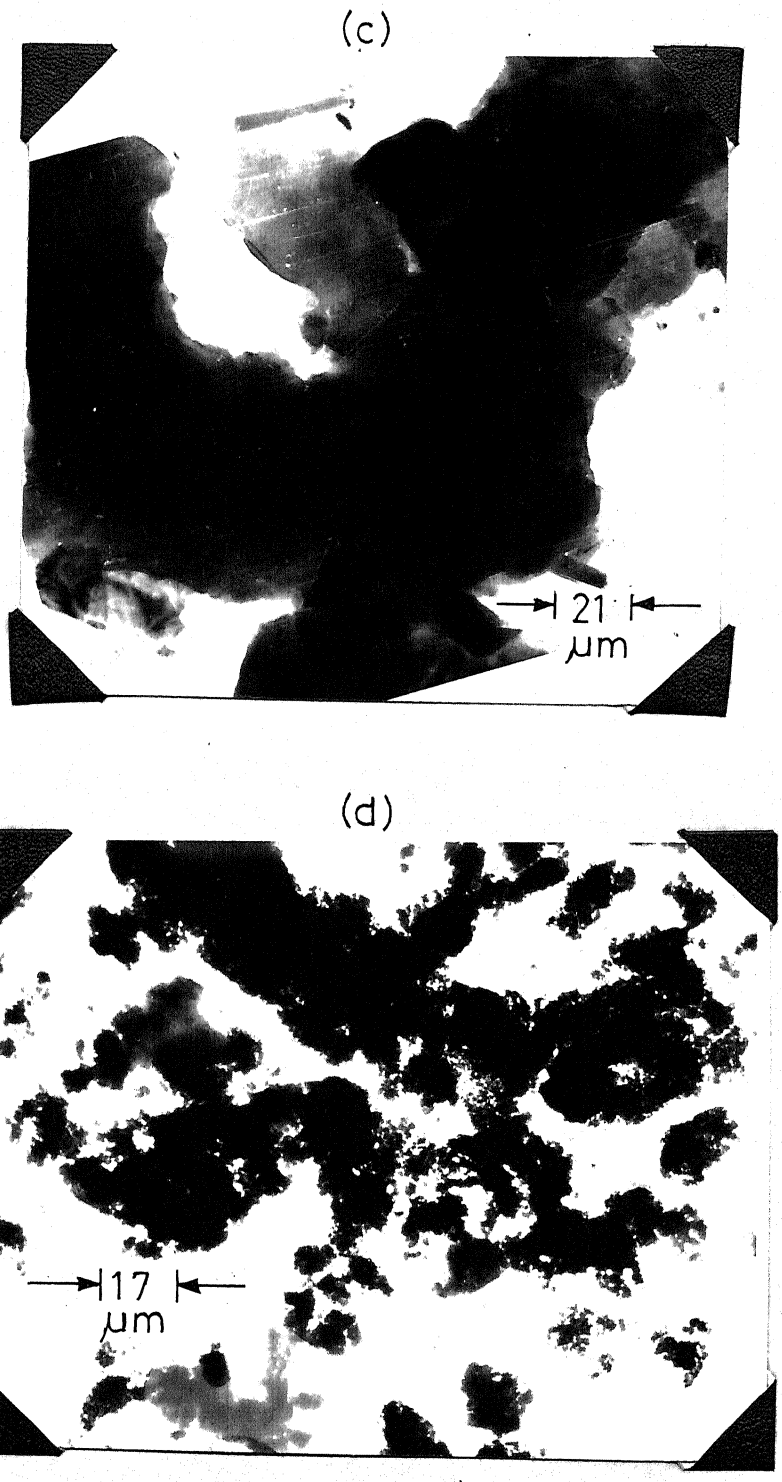

FIGURE 5: ELECTRON MICROGRAPH OF SINGLE GRAINS
(c) NiO-15-450-12
(d) NiO-20-450-12

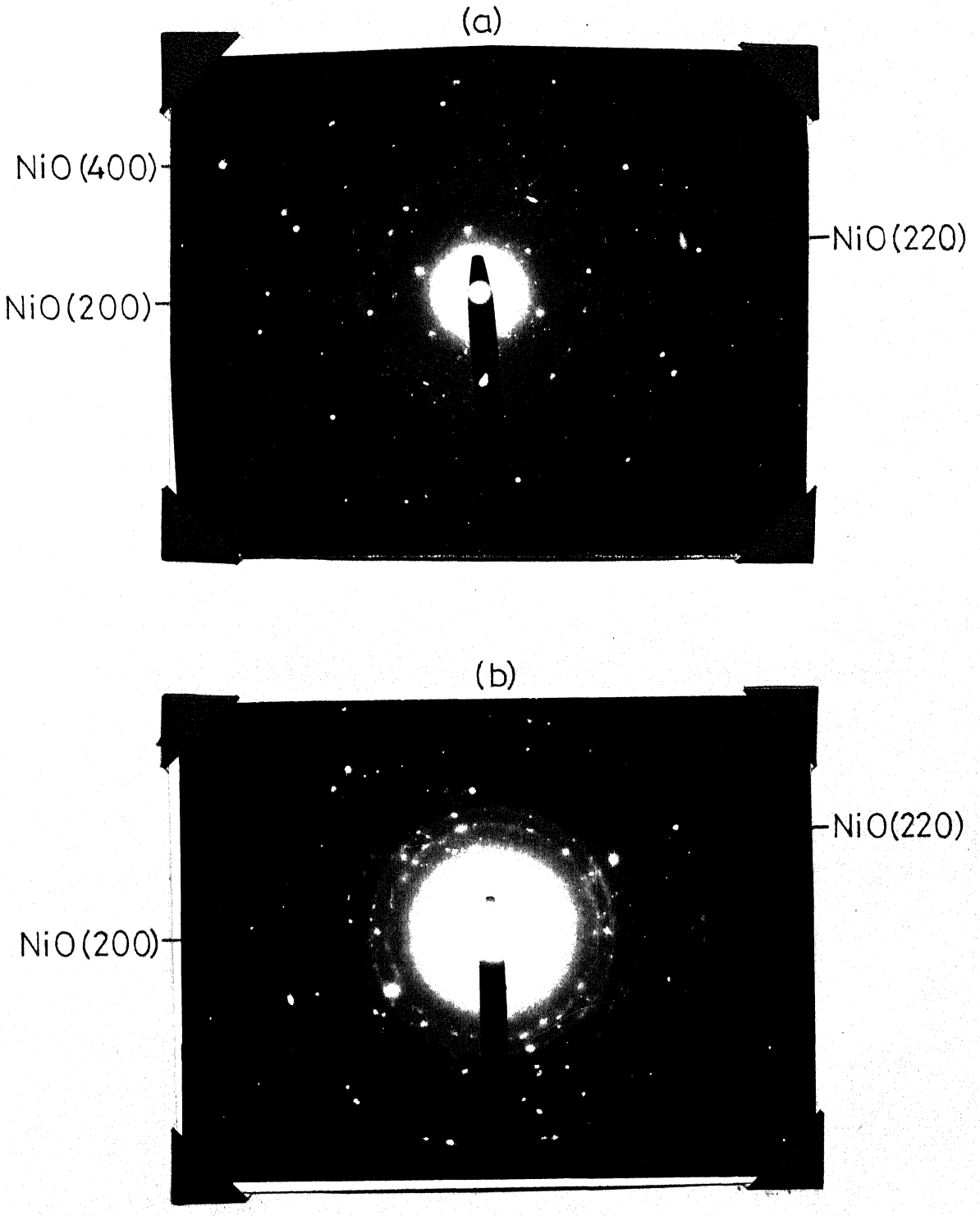

FIGURE 6: POWDER ELECTRON DIFFRACTION
(a) NiO-15-450-12
(b) NiO-20-450-12

It should be remembered that most intense lines from different aluminas including γ-Al_2O_3 emerge from almost the same Bragg angle. Thus any major alternations in structure of the alumina due to NiO can be followed by changes in electron diffraction intense lines. Figures7 **a and b** show the electron diffraction for pure alumina powder and 20 per cent NiO catalyst. No shift or change in pattern of alumina lines was obtained. Thus it is safe to conclude that alumina is not affected by NiO.

The electron micrograph of polycrystal grain of pure alumina, 10 per cent, 15 per cent and 20 per cent NiO are shown in Figure 8 a,b,c and d. The corresponding frequency distribution curves are shown in Figure 9 a,b,c and d, respectively. In all the cases majority of particles fall below 1 μm size. This is quite possible as the carrier alumina has itself majority of particles below 1 μm. In principle the impregnation of alumina by NiO should not affect the particle size of the support.

It is interesting to note that pore diameter of alumina support (Figure 4a) and the size of isolated particles (Figure 5a) of NiO-5-450-12 are almost equal. This indicates that at lower concentration the pores are coated first and then with increasing concentration the external surface, resulting in continuous coating. Finally many pores may be completely filled resulting into loss of physical surface area. This is verified by the decreasing trend of surface area with catalyst composition (Table 3).

(a)

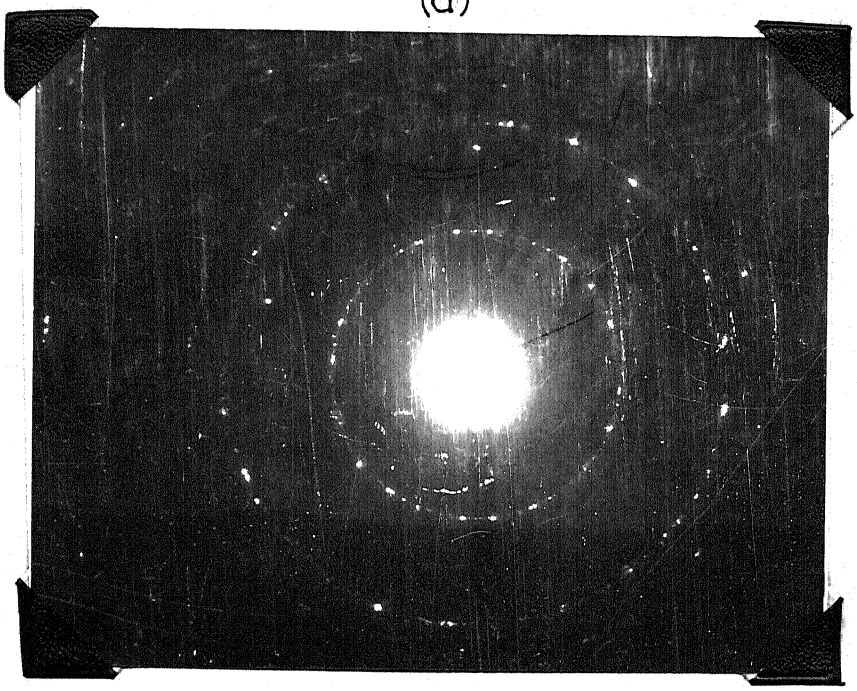

(b)

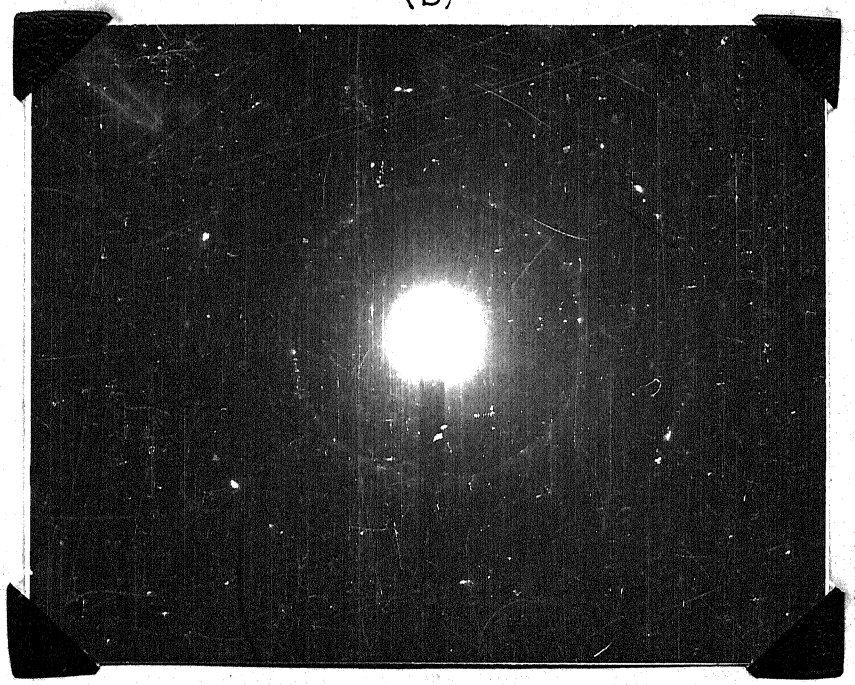

FIGURE 7: POWDER ELECTRON DIFFRACTION
(a) Pure γ-Al_2O_3
(b) NiO-20-450-12

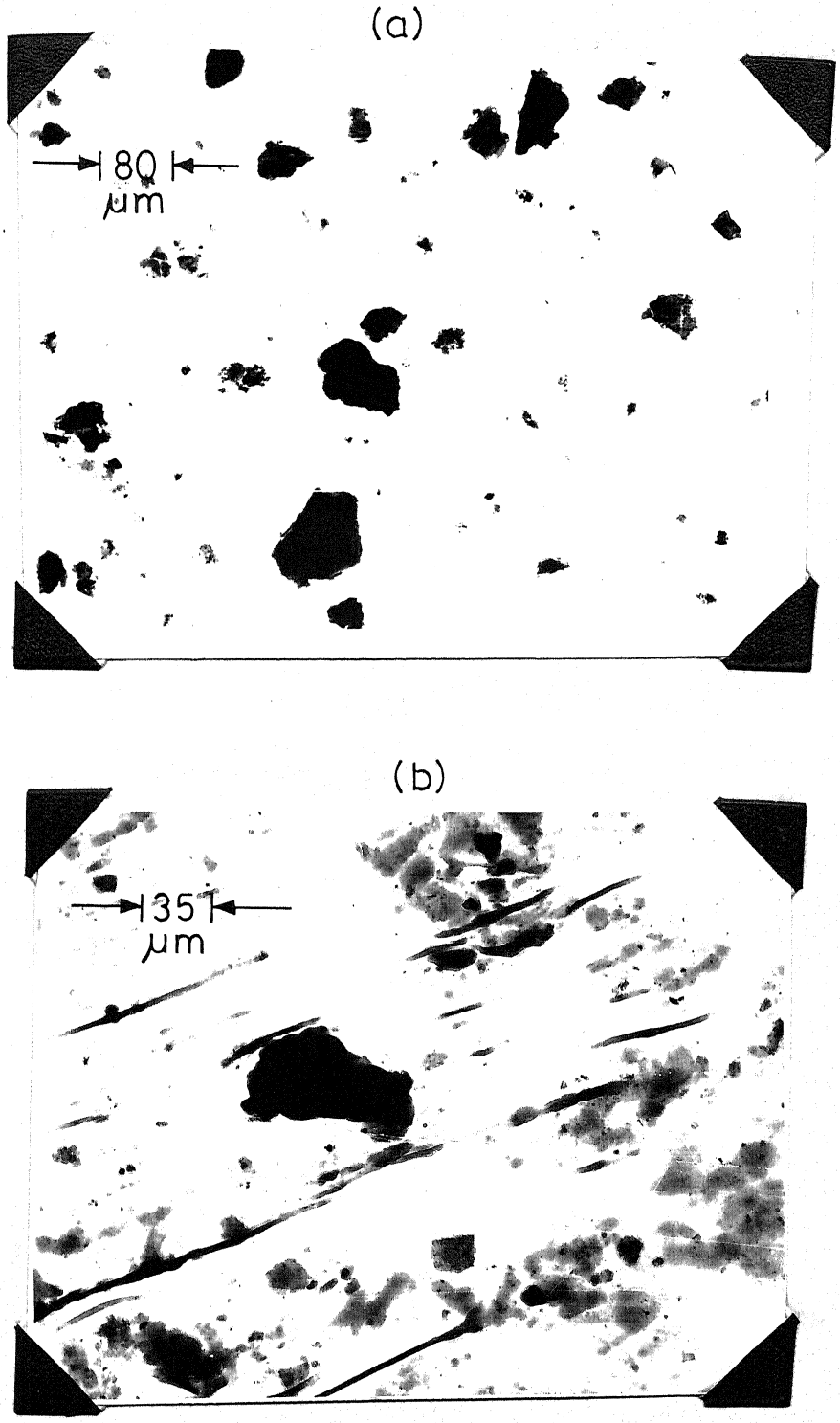

FIGURE 8: ELECTRON MICROGRAPH OF POLYCRYSTAL GRAINS

(a) Pure γ-Al_2O_3

(b) Ni0-10-450-12

(c)

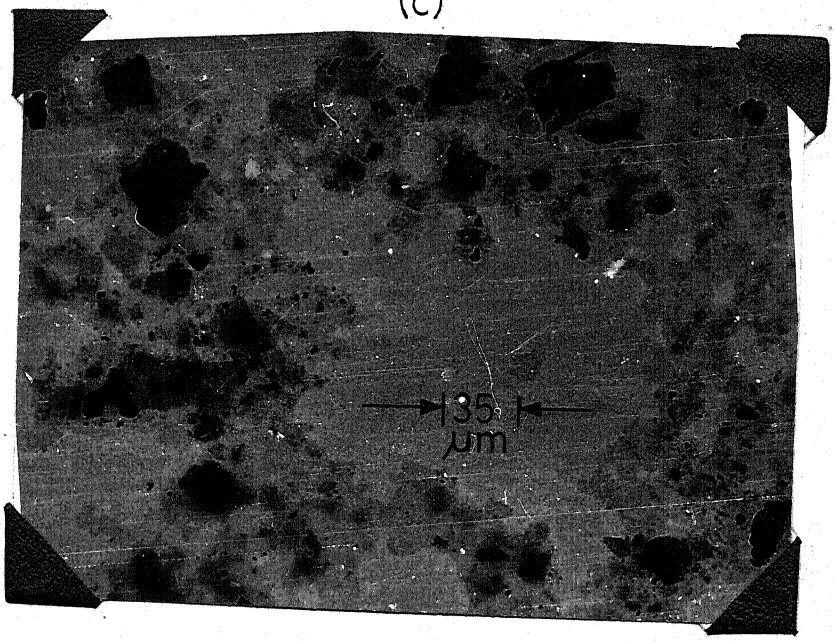

(d)

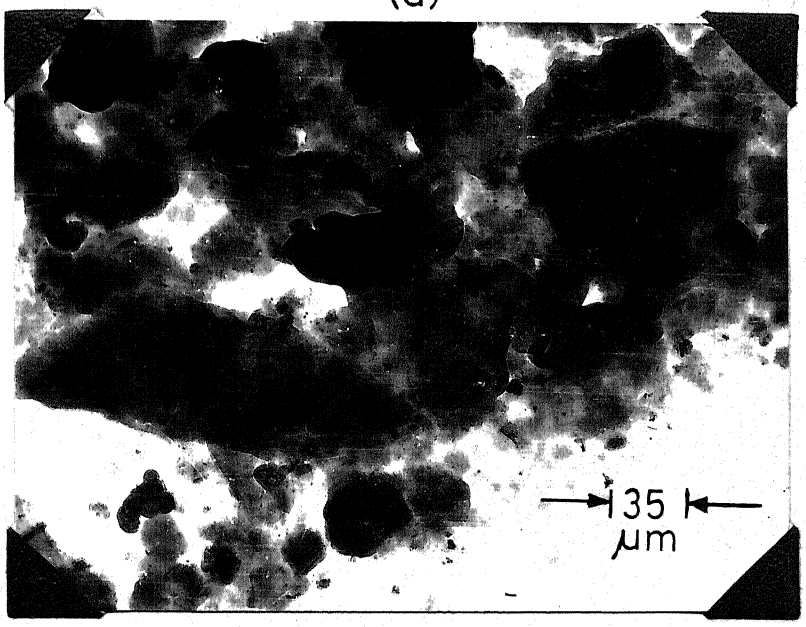

FIGURE 8: ELECTRON MICROGRAPH OF POLYCRYSTAL GRAINS

(c) NiO-15-450-12

(d) NiO-20-450-12

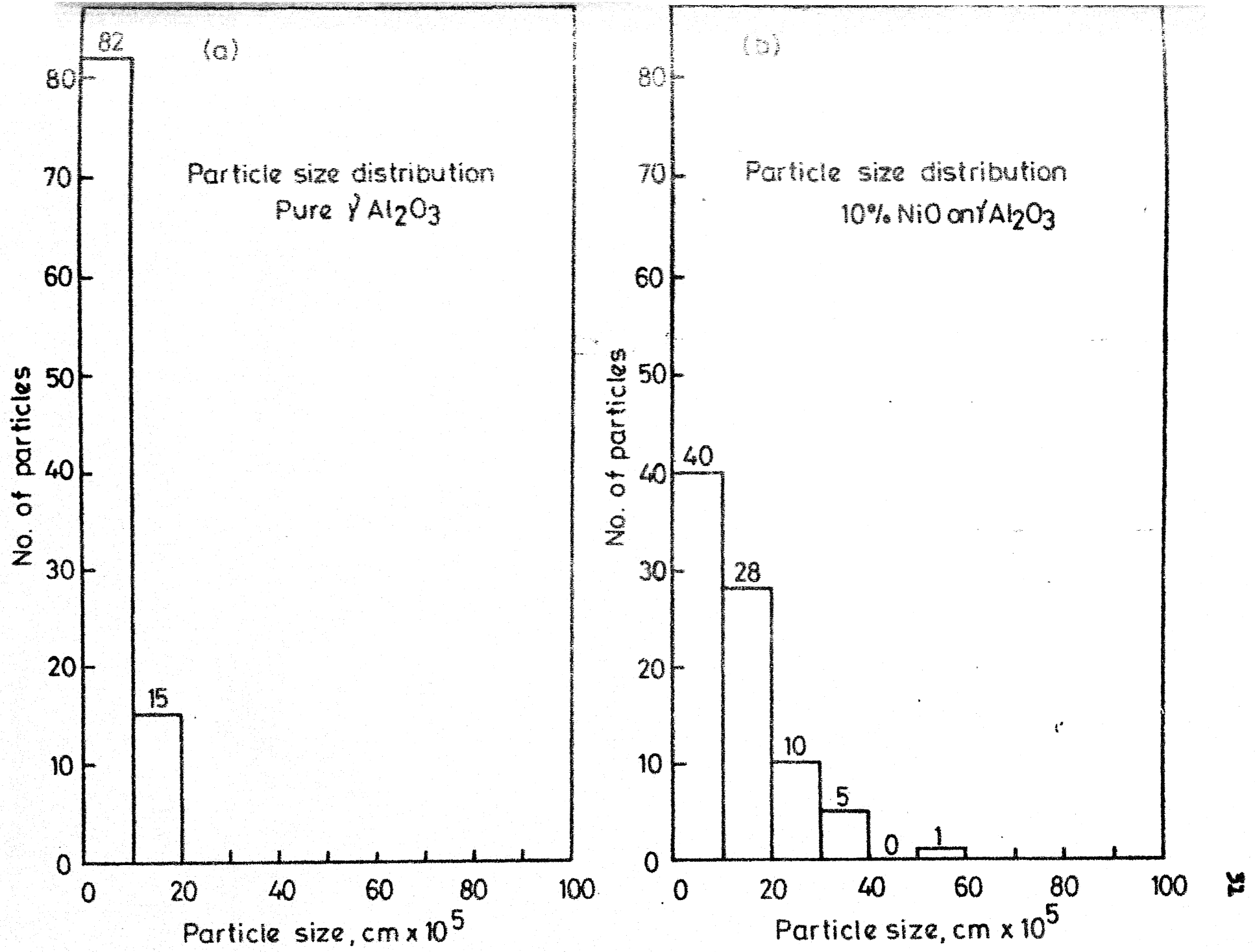

Fig. 9 - Frequency distribution curves.

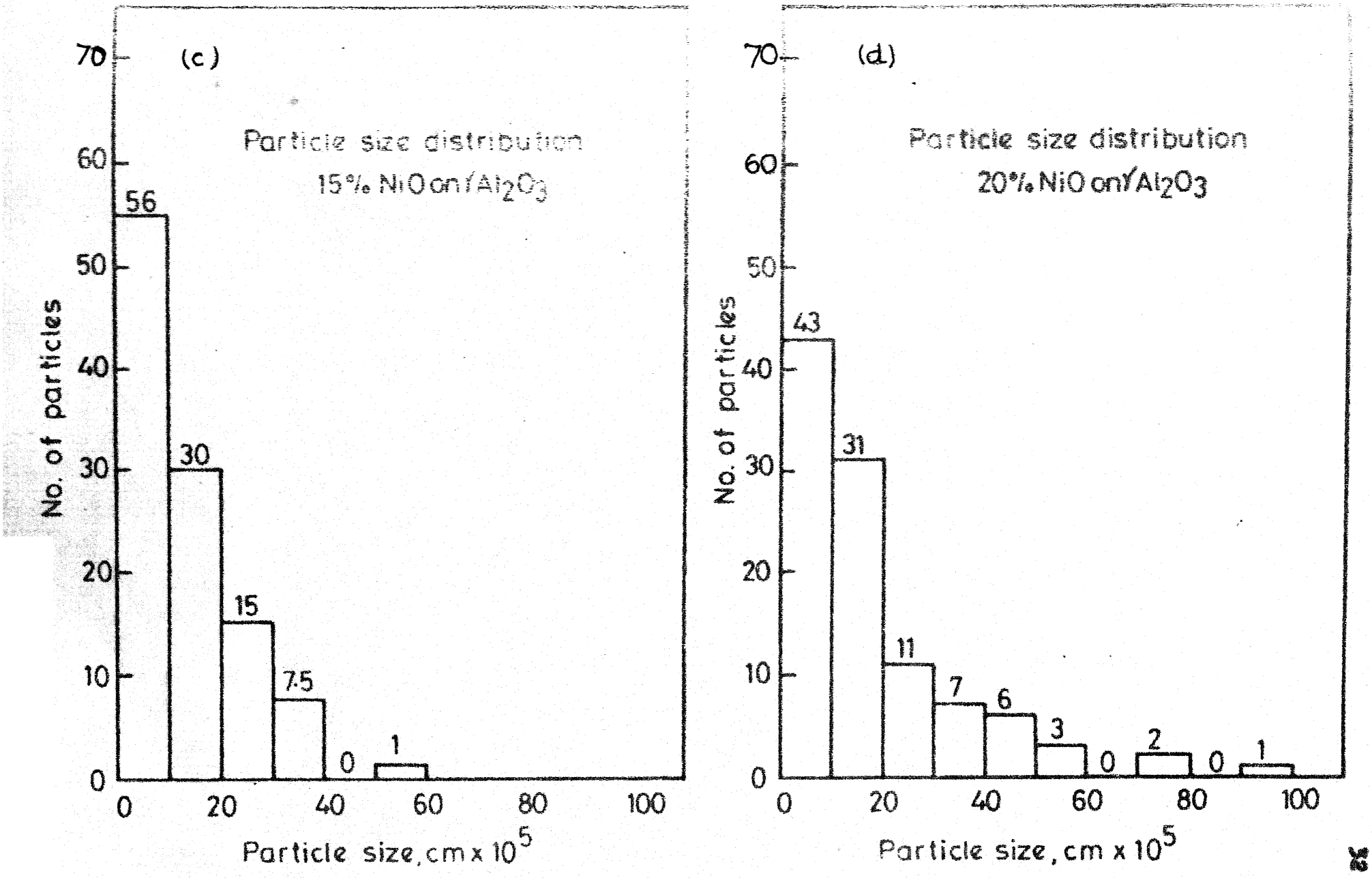

Fig. 9 - Frequency distribution curves.

1.4 CONCLUSIONS AND RECOMMENDATIONS

The salient findings of this study relative to NiO-Al_2O_3 systems are:

TG analysis showed a gradual loss in weight which was attributed to the release of excess oxygen which NiO contained.

The electron diffraction studies of commercial γ-Al_2O_3 showed that it contained, in small proportions other forms of aluminas. The alumina grains had interconnecting pores forming channels. The pore size was of the order of 50 Å. Neither alumina nor NiO were structurally affected by each other. This confirms the inertness of the alumina to NiO under the conditions of the system studied. In all the catalyst samples the majority of the support particle size was 1 μm. For 5 per cent NiO concentration the average particle size of NiO catalyst was 55 Å (NiO-5-450-12).

Evidence for the formation of nickel aluminate on the surface of alumina was not indicated by both X-ray and electron microscopic studies.

Valuable information might be obtained for this system from a study of the detailed heat treatment of the catalysts and its corresponding physico-chemical properties.

REFERENCES

1. Kurkova, N.S., Katsobashvilt, Ya. R., and Akchurina, N.A., Zh. Prikl. Khim. 46, 1003 (1973).
2. Gavrish, A.M., and Zoz, A., Chem.Abs. 77, 95531 (1972).
3. Umemura, K., Bulletin of Univ. of Osaka, Perfecture; Series A, 21, 321 (1972).
4. Domka, F., Dudzik, Z., and Gasiorek, M., Reaction Kinetics and Catalysis Letters.2, 171 (1975).
5. Katsobashivilt, Ya. R., Kurkova, N.S., Safanova, V.F., and Gracheva, T.A., Khim, Technol. Topl. Masel. 16, 1 (1971).
6. LoJacona, M., Schavello, M., and Cimino, A., J. Phy. Chem. 75, 1044 (1971).
7. Holm, V.C.F., and Clark, A., J.Catal. 11, 305 (1968).
8. Pillar, R.M., Carruthers, P.G., and Nutting, J., J. Mater. Science 2, 28 (1967).
9. Rubinshtein, A.M., Kinet. Catal., 8, 936 (1967).
10. Bousquet, J.L., Gravelle, P.C., and Turner, S.J., Bull. Soc. Chim. Fr. 7, 2229 (1969).
11. Richardson, J.T., and Milligan, W.D., J. Phy. Chem. 60, 1223 (1956).
12. Andrew, S.P.S., 'Preparation of Catalysts', Ed. Delmon, B., Jacobs, P.A., and Poncelet, G., Elsevier, Amsterdam, 429-444 (1976).
13. JoseCervello, J.F., Garcia, E.H., and Jimenez, J.F., Chem. Ing. Tech. Jahrg. 48(b), 520 (1976).

14. Emmett, P.H., 'Catalysis Vol. I', Reinhold Publishing Co., Inc., New York (1966).

15. X-ray powder diffraction data file, ASTM 4-0835, ASTM. 10-425, (1966).

16. Yao, H.C., and Shelf, M., 'The Catalytic Chemistry of Nitrogenoxides', Ed. Klimisch, R.L., and Larson, J.G., Plenum, New York (1975).

17. Krischner, H., Porkar, K., and Donnert, D., Ber. Deut. Keram. Ges. 46, 240 (1963).

18. Nokamoto, K., 'Infrared spectra of Inorganic and Coordination Compounds', John Wiley, New York (1970).

19. Agarwal, A.K., and Srivastava, R.D., J.Catal. 45, 86 (1976).

20. LeBlanc, Von. M., and Sachse, H., Z.Elektrochem. 32, 204 (1926).

21. Prasad, M., and Tendulkar, M.G., J.Chem.Soc. 1403 (1931).

22. Tsuchida, T., Furuichi, R., and Ishii, T., Z. Anorg. Alleg. Chem. 415, 175 (1975).

SECTION 2

CATALYTIC ACTIVITY OF NiO-Al_2O_3 SYSTEMS

CONTENTS

LIST OF FIGURES

LIST OF TABLES

NOMENCLATURE

F	Flow rate of feed, moles/hr
W	Weight of catalyst, g.
P	Total pressure, atm
p	Partial pressure, atm.
R	Gas constant K.cal/(mole)(^{o}K)
T	Temperature, ^{o}K

Greek Symbols

α, γ, η	Different phases of alumina

2.1 INTRODUCTION

Catalysts based upon $NiO-Al_2O_3$ are remarkable for the multiplicity of the reactions they promote: these include reforming of hydrocarbons, hydration, dehydration, hydrogenation, dehydrogenation, oxidation and reduction. The mechanism of decomposition of cyclohexanol over $NiO-Al_2O_3$ is quite unclear with respect to nature of adsorbed species and with active centres of the catalyst.

Paal et al. [1] and Lyubarskii and Strelets [2] investigated the reactions of cyclohexanol in the presence of a carrier free nickel catalyst. The main reaction was dehydrogenation giving cyclohexanone. This later suffered further transformation into phenol. By means of radioactive tracers it has been shown that no direct dehydrogenation of the saturated C_6 ring took place. Radiotracer studies also showed no direct hydrogenolysis of cyclohexanol.

Tetenyi and Schachter [3] studied the dehydrogenation of cyclohexanol at 235°C over Fe, Ni, Co, Cu and Pt catalysts For the Fe, Co, Ni and Pt catalysts cyclic hydrocarbons were also formed mainly because of the hydrogenation or dehydrogenation of cyclohexene produced by the dehydration of cyclohexanol. For Ni, Fe and Pt the rate of desorption of cyclohexene was slower than that of the transformation of cyclohexene to benzene. At 235°C the dehydrogenation of cyclohexanol was much slower.

It has been shown by radiotracer studies [4] that in the presence of copper and nickel, cyclohexanol gives phenol exclusively via cyclohexanone whereas in the presence of Pt there is a direct pathway for the dehydrogenation of cyclohexanol into phenol.

The effect of nickel crystal size on catalytic activity of nickel supported on silica-alumina using ethane hydrogenolysis as the test reaction was investigated by Carter et al. [5]. It was found that the catalytic activity of nickel decreased with increasing crystallite size to a larger extent. The specific catalytic activity of nickel thus decreased as the crystallite size increased.

Krawezykova et al. [6] studied the rate of dehydrogenation of cyclohexanol to cyclohexanone over Ni-Al_2O_3 at 170°C. It was found that the rate was greater in the presence of phenol than in its absence and reached a maximum at a phenol concentration of 30 per cent. Increasing the catalyst concentration from 1 to 5 per cent increased the rate of reaction only slightly.

Edwige et al. [7] reported that the dehydrogenation of cyclohexanol to cyclohexanone on NiO starts at 220°C and is 96 per cent completed at 450°C. A small amount of cyclohexene is formed at 250-300°C. In the dehydrogenation of cyclohexanol, 31 to 48 per cent Ni on Al_2O_3 gives only cyclohexene, but with 70 per cent Ni on Al_2O_3 approximately 5-6 per cent

cyclohexanone is formed. On Al_2O_3-85 per cent NiO catalyst, 40 per cent cyclohexanone is formed at 400°C.

The results of comparative study of nickel oxide - alumina and nickel oxide - silica-alumina catalysts [8] in the light of the characteristics of the support systems alumina and silica-alumina showed that the impregnation of NiO does not produce any significant change in the textural characteristics like surface area and pore volume of the support oxides. The activation energies for dehydrogenation and dehydration are 21.2 and 11.2 KCal $mole^{-1}$, respectively.

Skrigan [9] reported that with maximum concentration 12.1 per cent Co on MgO catalyst rate of dehydrogenation of cyclohexanol to cyclohexanone at 235-285°C increased linearly with contact time indicating a diffusion controlled reaction.

Belskaya et al. [10] studied the dehydrogenation of cyclohexanol on Cu/Al_2O_3. They reported that to increase the activity and selectivity of a catalyst as well as its stability the **title** catalyst contains 15-25 per cent of Cu and promotor K_2O 1-3 per cent on a support consisting of fibrous alumina.

The dehydrogenation of cyclohexanol in a fixed bed of catalyst in the temperature range of 210-300°C using the catalyst (Cu, 47; Ni, 47; Cr_2O_3, 4; K_2O, 1 and U, 1 per cent) was studied by Pillai and Kuloor [11]. The data are expressed in the form of first order forward and second order backward rate equations.

Straszko [12] described extensive studies on the catalytic activity and the physico-chemical properties of binary and ternary systems such as NiO/Al_2O_3, Ni/SiO_2, Ni/MgO, NiO/Al_2O_3 and $Ni-CO/Al_2O_3$. The structure of the catalyst carrier was established by ir and X-ray methods. The structure of the deposited substances was determined by X-ray methods only. To determine the catalytic properties of each catalyst system its effect on the decomposition of isopropyl alcohol and on the hydrogenation of benzene was examined.

Schiavello et al. [13] tested the catalytic properties of samples of $Ni^{2+}/\gamma-Al_2O_3$ and $Ni^{2+}/\eta-Al_2O_3$ prepared in damp and in dry atmosphere for N_2O decomposition. The results are interpreted in terms of the different $[Ni^{2+}]$ oct/$[Ni^{2+}]$tet ratio present in the various types of catalyst. It was shown that nickel ions exposed from octahedral sites $[Ni^{2+}oct]$ are more active than those exposed from tetrahedral ones $[Ni^{2+}$ tet]; hence a high catalytic activity parallels a high $[Ni^{2+}$ oct]/$[Ni^{2+}$ tet] ratio.

Yasumura and Yoshino [14] studied the specific activity of dehydrogenation of cyclohexanol at 200-375°C over Raney-Cu catalyst. The most active composition was 40 per cent. When the alloy content was 80 per cent the catalyst showed dehydration properties. At temperatures greater than 300°C the amount of cyclohexene and water was increased in the reaction products.

The dehydrogenation of cyclohexanol to cyclohexanone using $Ni-Al_2O_3$ catalyst with added Pt, KOH, Na_2SO_4 and Cr_2O_3 showed that Cr_2O_3 had the greatest promoting ability and Pt the weakest. Na_2SO_4 increased the selectivity of the process [15].

Skrigan and Dmitrieva [16] studied the catalytic activity of Cu applied on different supports ($\gamma-Al_2O_3$, $\alpha-Al_2O_3$, MgO, $MgAl_2O_4$, $ZnAl_2O_4$, ZnO, BeO, SiO_2 and ZrO_2) in the dehydrogenation of cylohexanol. Maximum activity was observed in the case of $\gamma-Al_2O_3$ support. The catalytic conversion of cyclohexanol at 150-360°C on Cu, Ni and Pt catalysts showed that dehydrogenation proceeded with all of the catalysts [17]. On Cu cyclohexene was not converted any further. On Pt and Ni catalysts cyclohexane and benzene were formed from cyclohexene.

From the literature review it is evident that there appears to be no prior detailed study where $NiO-Al_2O_3$ system was correlated with its activity for cyclohexanol decomposition. This prompted us to undertake this investigation to correlate solid state properties of a series of impregnated $NiO-Al_2O_3$ samples to its catalytic activity. Extensive use of various techniques have led to considerable insight into the crystal size and specific surface as discussed in Section 1.

The principal aim of this work is to examine the effects of several variables such as catalyst composition, reaction temperature, concentration of products of decomposition and especially to evaluate the role of active element and the

support in the mechanism of reaction. Studies of this type are expected to lead to a better understanding of the nature of active sites in relation to catalytic activity. Cyclohexanol which may react in different directionsis a very interesting substrate for the study of preferred reaction pathways and their possible explanation .

2.2 EXPERIMENTAL

2.2.1 Catalyst Preparation

The preparation of supported NiO catalysts containing upto 20 weight per cent NiO calcined at 450°C for 12 hours and their characterization along with details of measurement of particle size distribution and crystal growth have been discussed in Section 1.

2.2.2 Apparatus and Procedure

A schematic diagram of the experimental set-up for the catalytic vapour phase decomposition of cyclohexanol is given in Figure 1. The cyclohexanol was fed by the calibrated metering pump into a preheater where it was vapourized. The vapour was then led to the reactor containing the catalyst. The reactor was partially filled with porcelain beads to support the catalyst as well as to ensure uniform distribution of the reactant vapours. Besides, it helps the preheated reactant to attain the reaction temperature.

The temperature in the catalyst bed was measured with an iron-constantan thermocouple located in a coaxial thermowell. Temperature control was achieved by diluting the catalyst with inert porcelain beads in the ratio of 1:5 by volume. The main stream of the effluents from the reactor was cooled by condenser. The liquid condensate was analysed by the gas chromatography and the gaseous products were metered.

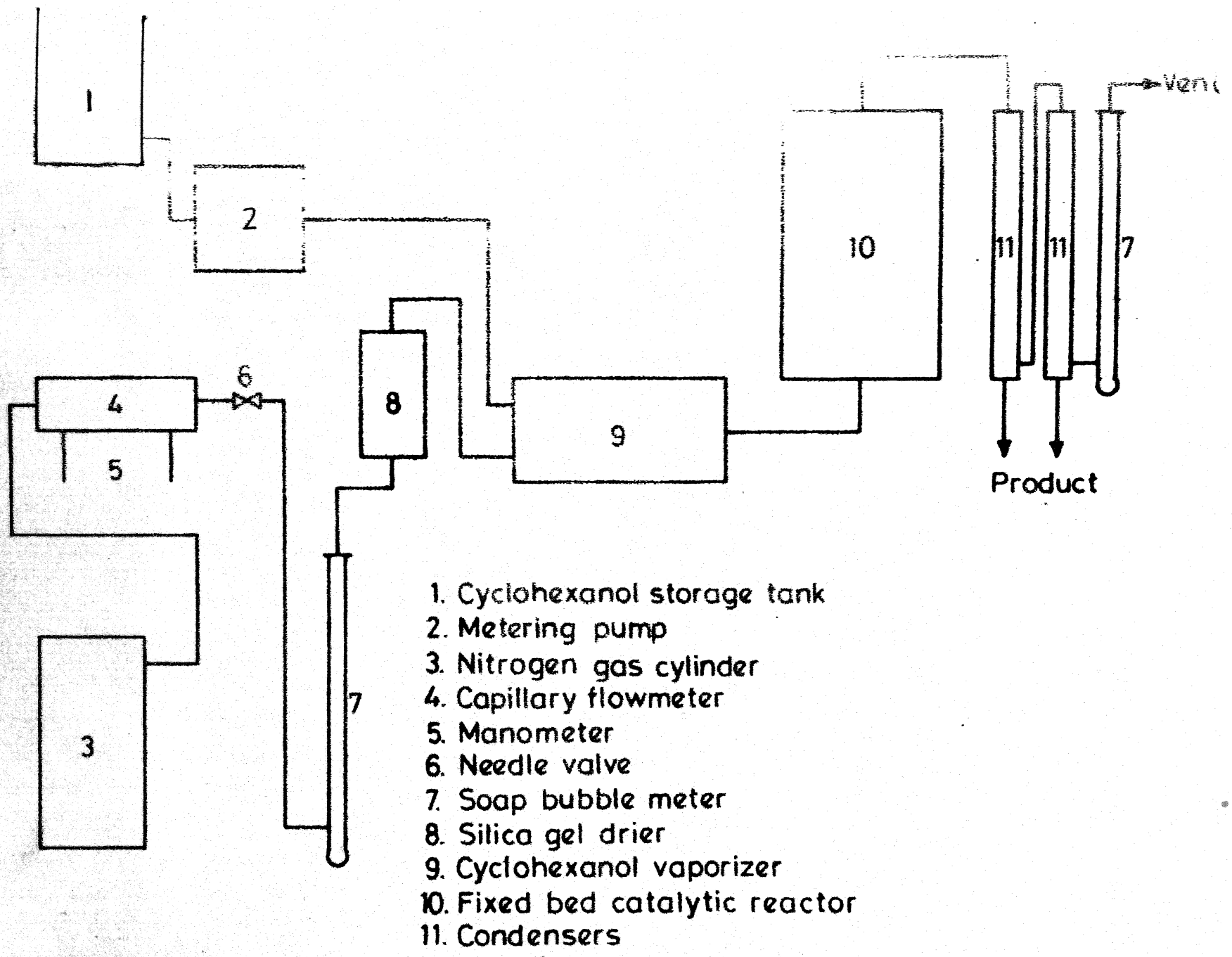

Fig. 1 - Schematic diagram of the experimental setup.

2.2.3 Analytical Technique

The analyses were performed by employing a C.I.C.A.C. gas chromatograph provided with a thermal conductivity detector, oven and injector. The output response of the chromatograph was recorded on a Honeywell recorder.

A 254 mm long and 12 mm diameter copper tube packed with 20 per cent carbowax 20-M on Chromosorb.P. (30-100 mesh) was used as an analysing column in the chromatograph. Nitrogen was used as carrier gas (60 ml min^{-1} flowrate). The temperature of the detector and injector blocks were maintained at 250°C and 220°C respectively. The temperature of the oven was kept constant at 160°C. Sample size of 10 µl was used.

2.3 RESULTS AND DISCUSSION

Experimental reaction data were obtained on a series of catalyst at a constant W/F = 50 g.hr.mole^{-1} in the temperature range 300-450°C. All determinations were made within one hour after activation of catalyst. After steady state was attained 7 analyses were made in 30 minutes intervals. The average of the last two values of these analyses was used for the estimation of conversion. The catalytic activity was defined as the number of moles of cyclohexanone formed per unit time per unit weight of catalyst (moles hr.$^{-1}$ g.$^{-1}$). Reference to various samples will be made as discussed in Section 1. Initial runs, carried out with pure γ-Al_2O_3 under identical conditions, indicated that γ-Al_2O_3 was acting as a dehydrating catalyst. The analysis of the products gave no indication of the formation of cyclohexanone.

Figure 2 shows the variation of activity as a function of temperature for various catalyst compositions. In all the cases, the pattern of the plots was the same. The maximum activity was obtained with NiO-15-450-12 catalyst. It is also evident from Figure 2 that the activity increases with temperature and passes through maximum at a temperature of 350°C. This is possibly due to the change in mechanism of the reaction. To decide this aspect further, a complete

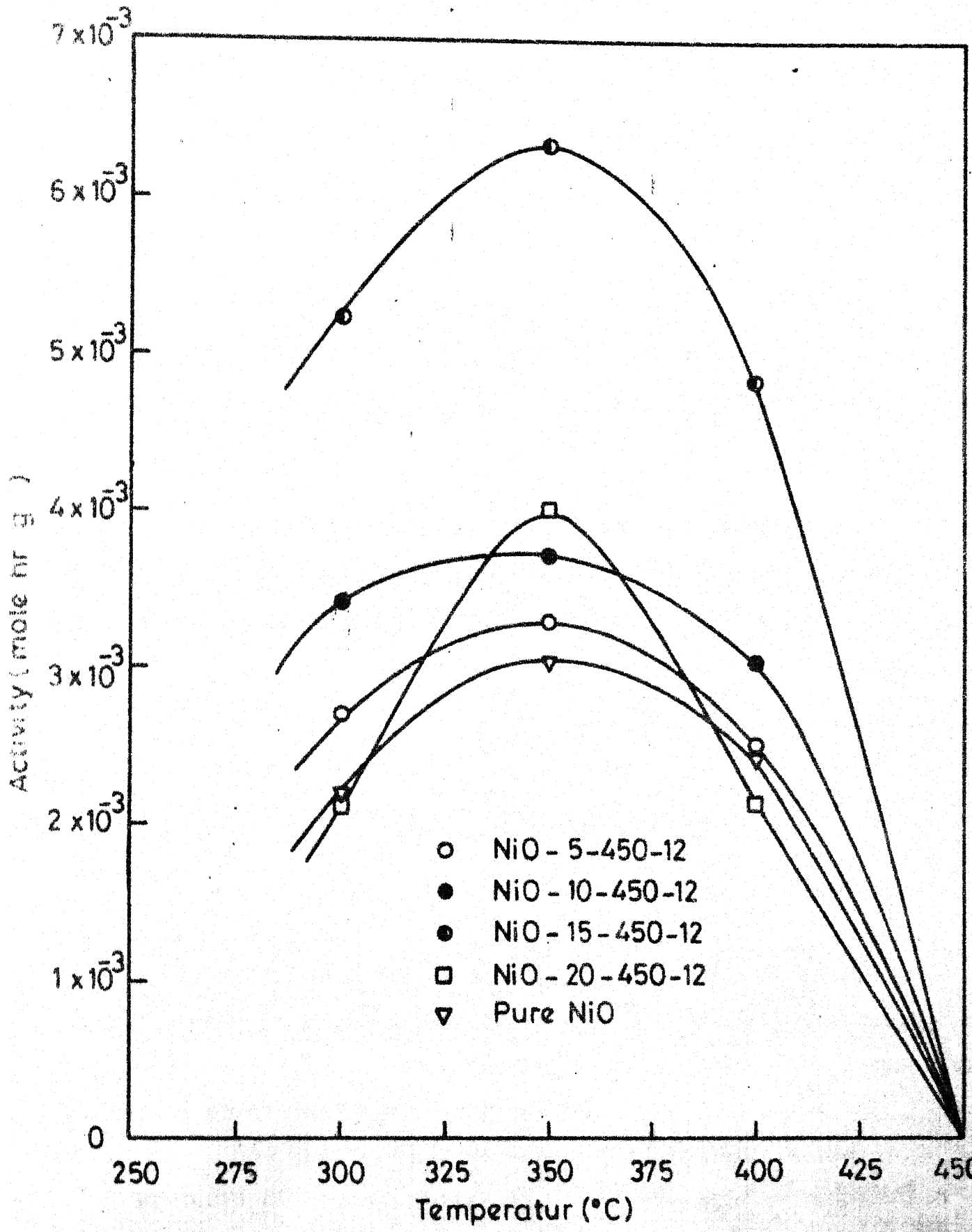

Fig.2-Catalytic activity of $NiO-Al_2O_3$ for cyclohexanol dehydrogenatio at various temperatures. W/F=50 g hr mole^{-1}

product analyses were made at all temperatures. These results are given in Table 1.

It follows from the experiments presented that, in the studied $NiO-Al_2O_3$ system, the influence of both the components becomes evident in its structural properties. The found dependence of catalytic activity (Figure 2) is typical for a modified surface of the catalyst. It is analogous to the dependence found for the $NiO-Al_2O_3$ system using N_2O decomposition [13], where the authors explain the obtained course by the presence of surface spinel. In our case, the electron microscopy and X-ray analysis of the samples (Section 1) did not reveal the formation of the 'surface spinel' ($NiAl_2O_4$) and the observed dependence seems then little probable to be explained in this way.

The phenomena observed can be explained by the influence of the degree of dispersion of the active component as well as by the stoichiometric excess amount of oxygen present in the catalyst samples. As has been discussed in Section 1, the presence of excess oxygen in the NiO-15-450-12 and in NiO-20-450-12 catalyst samples are indicated by the black color of the catalyst which may be important for the catalytic activity of NiO. This suggests that Ni^{+++} ions are responsible for the catalytic activity of NiO.

The electron microscopic analyses detected the presence of crystal growth of NiO on the alumina support.

TABLE 1: PRODUCT DISTRIBUTION AT DIFFERENT TEMPERATURES (MOLE PER CENT)

Temperature °C	C_6H_{10}	C_6H_6	$C_6H_{10}O$	$C_6H_{11}OH$	H_2O	H_2
			NiO-5-450-12			
300	37.6	2.1	7.0	2.5	39.7	11.2
350	35.7	2.6	8.2	1.8	38.3	13.4
400	36.2	3.5	6.3	1.0	39.7	13.4
450	40.2	4.7	0.0	0.7	44.9	9.4
			NiO-10-450-12			
300	30.8	4.3	8.2	4.8	35.1	16.8
350	29.2	5.5	8.6	2.4	34.6	19.6
400	30.7	6.1	6.4	1.4	36.8	18.5
450	34.3	7.4	0.0	1.8	41.7	14.8
			NiO-15-450-12			
300	25.4	5.2	12.4	3.8	30.6	22.7
350	17.3	9.2	13.5	1.8	26.5	31.8
400	8.1	19.5	2.6	0.4	27.7	41.7
450	8.0	21.0	0.0	0.3	28.9	41.9
			NiO-20-450-12			
300	38.1	3.3	5.3	3.3	41.4	8.4
350	24.7	7.5	8.9	2.7	32.2	23.9
400	11.6	16.8	3.8	2.1	28.3	37.4
450	9.9	19.6	0.0	1.8	29.5	39.2

only in the case of NiO-20-450-12 catalyst. A correlation with solid state properties may also be derived from the observation of close correspondence between the crystallite size (Figure 5.d of section 1) and catalytic activity (Figure 2). On this basis, one is entitled to conclude that the catalytic activity decreased with increasing crystallite size to a larger extent than could be accounted for by the corresponding decrease in surface area. The surface area varied from 96 to 77 m^2g^{-1}. (Table 3, Section 1). The catalytic activity is also known to decrease with the increase in particle size of catalyst. For the particles below 1 μm the number of particles are maximum in the case of NiO-15-450-12 catalyst than NiO-5-450-12, NiO-10-450-12 and NiO-20-450-12 as discussed in Section 1 (Figure 9 (a-d)).

Carter et al. [5] investigated the effect of nickel crystallite size on the catalytic activity of nickel supported on alumina using ethane hydrogenolysis as a test reaction. They also reported that the catalytic activity of nickel was decreased as the crystallite size increased. The decrease in catalytic activity could not be accounted for by the corresponding decrease in surface area.

At the outset of this part of the discussion it should be made clear that the main object of this study was to measure the product distribution and to deduce therefrom the possible reaction paths. The results of the product

distribution (Table 1) show the existence of two distinct regions in the $NiO-Al_2O_3$ systems: parallel dehydrogenation and dehydration in the low temperature region (300-350°C) and consecutive dehydration and dehydrogenation of cyclohexanol in the high temperature region (350-450°C). The direct dehydrogenation activity of cyclohexanol changes more drastically above 350°C though the variation is much more smaller with the content of active phase in the catalyst (Table 1). This is in good agreement with the previous work [6,7] where the authors reported same amount of cyclohexanone in the temperature range studied.

Passing cyclohexanol over all the catalysts below 350°C, less than 10 mole per cent of benzene was detected. More benzene was formed at higher temperatures. This suggests that at higher temperatures cyclohexene adsorbs in the form of benzene and hydrogen. Similar results have also been reported in the literature with other catalysts for this type of reaction [14, 17-18].

The formation of benzene may also be possible through hydrogenolysis of cyclohexanol, however a separate experiment with cyclohexene in the absence of cyclohexanol showed that benzene is produced only through cyclohexene. Radiotracer studies proved no direct hydrogenolysis of cyclohexanol [1,2].

Studies conducted with pure γ-Al_2O_3 in the temperature range of 300-450°C showed the presence of cyclohexane, cyclohexene, benzene, water and hydrogen. As has been said in the beginning of this section, no cyclohexanone was detected in the products. The predominant reaction is the cyclohexanol dehydration followed by hydrogenation and dehydrogenation of cyclohexene. Between 300-350°C cyclohexane was around 30 mole per cent whereas benzene was less than 10 mole per cent. The cyclohexene mole per cent decreased from 50 to 30 as the temperature was increased. It was also observed that above 350°C no cyclohexane was formed, however, the formation of benzene from the particular cyclohexene increased rapidly. This suggests that at low temperature the dissociated hydrogen apparently can migrate to the other benzene/cyclohexene molecules and hydrogenates them to cyclohexane, since the desorption of benzene was more difficult at these temperatures.

On the basis of the above mentioned evidences the following reaction scheme may be postulated in the presence of NiO-Al_2O_3 catalyst (Figure 3).

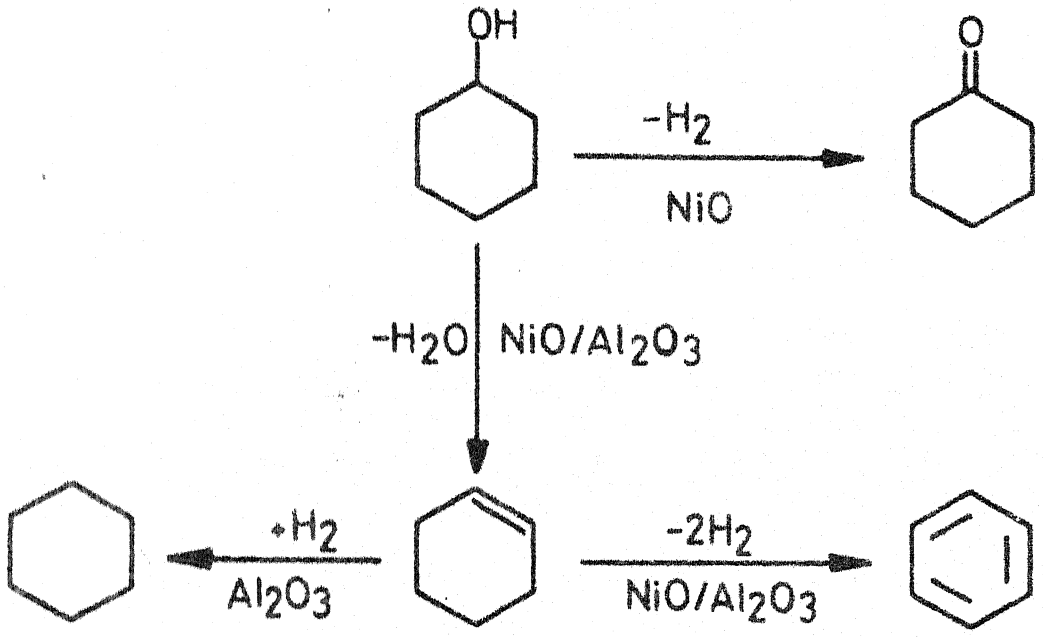

Fig. 3 - Different possible reation pathways.

This sequence valid for $NiO-Al_2O_3$ cannot be generalised for other catalysts where - due to different nature of active sites on the catalyst surface other processes or other reactions may be found.

2.4 CONCLUSIONS AND RECOMMENDATIONS

This study leads to information on the following points:

The decrease in catalytic activity in the case of NiO-20-450-12 catalyst may be accounted for the crystal growth of NiO on the alumina support.

The maximum activity was obtained with NiO-15-450-12 catalyst. This may be due to the presence of maximum number of particles below 1 μm size.

The results of catalytic activity prove undoubtedly the existence of two distinct regions in the NiO-Al_2O_3 systems: low temperature (300-350°C) region exhibits a high activity for direct dehydrogenation of cyclohexanol; high temperature region (350-450°C) exhibits a high activity for consecutive dehydration and dehydrogenation of cyclohexanol.

The present study indicates that the mechanism of cyclohexanol decomposition is much more complex than had been recognized. Further studies should be conducted at the catalyst calcined much above 450°C to avoid the existence of two distinct phases in the crystal lattice.

REFERENCES

1. Paal, Z., Peter, A., and Tetenyi, P., Z. Phy. Chemie N.F. 91, 54 (1974).
2. Lyubarskii, G.D., and Strelets, M.M., Khim. Prom. 43, 481 (1967).
3. Tetenyi, P., and Schachter, K., Acta. Chim. Acad. Sci. Hung. 65, 253 (1970).
4. Paal, Z., Peter, A., and Tetenyi, P., Reaction Kinetics Catalysis Letters. 1, 121 (1974).
5. Carter, J.L., Cusumano, J.A., and Sinfelt, J.H., J.Phy. Chem. 70, 2257 (1966).
6. Krawczykova, N., Ciborowski, S., and Crzelewski, L., Symp. Tspolz. Metod. Mechenykh At. Soversh. Technol. Protsessov Proizvod. Primen Yad-Fiz. Metod. Anal. Sostava Veshchestva 1968 (Pub. 1969), 144-150 (Russ), C.A. 73, 119904V (1970).
7. Edwige, G., Michele, P., and Roger, G., Bull. Soc. Chim. (Fr.) 8, 2882 (1970).
8. Viswanathan, V.N., and Yeddanapalli, L.M., Z. Anorg. Allg. Chem. 407, 98 (1974).
9. Skrigan, E.A., Vestsi Akad. Navuk. Belarus SSR., Ser. Khim. Navuk, 3, 50 (1973); C.A. 79, 52585V (1973).
10. Bel'skaya, R.I., Berezovik, G.K., Novitskii, V.F., Ermolenko, I.N., and Sviridova, R.N., Otkrytiya, Izobret. Prom. Obraztsy, Tovarnyeznaki 53, 7 (1976); C.A. 85, 131278z (1976).

11. Pillai, T.J.R., and Kuloor, R., Ind. J. of Technol. 12, 327 (1974).

12. Straszko, J., Zesz. Nauk. Poltech. Szczecin, Pr. Monogr. 57, 7-126(Pol) (1969); C.A. 73, 91863E (1970).

13. Schiavello, M., LoJacona, M., and Cimino, A., J. Phy. Chem. 75, 1051 (1971).

14. Yasumura, J., and Yoshino, T., Kogyo. Kogaku Zasshi, 69, 1868 (1966).

15. Kozlov, N.S., and Skrigan, E.A., Zh. Prikl. Khim. (Leningrad) 48(9), 2097 (1975).

16. Skrigan, E.A., and Dmitrieva, L.P., Vestsi. Akad. Navuk. Belarus. SSR. Ser. Khim. Navuk. 2, 56 (1973) (Belorussian).

17. Manninger, I., Peter, A., and Paal, Z., Khem. Kozl. 44(1-2), 35 (1975).

18. Weisz, P.B., and Parter, C.D., Adv. in Catal. 6, 144 (1954).

SECTION 3

KINETICS OF PARALLEL DEHYDROGENATION AND DEHYDRATION OF CYCLOHEXANOL ON $NiO-Al_2O_3$ CATALYST SYSTEMS

CONTENTS

LIST OF FIGURES

LIST OF TABLES

NOMENCLATURE

A	Cyclohexanol
H	Hydrogen
K_1	Rate constant, (g.moles)/(hr.)(g.)
K_1^o	Arrhenius rate constant, (g.moles)/(hr)(g.)
K_i	Adsorption equilibrium constant for component, i, atm^{-1}
K_i^o	Arrhenius adsorption constant for component, i, atm^{-1}
n	Total number of data points
p_i	Partial pressure of component i, atm
Kl	Cyclohexanone
R	Gas constant, (cal.)/(g.mole)(^oK)
r	Experimental reaction rate, (g.moles)/(hr)(g)
$\hat{r}$	Calculated reaction rate, (g.moles)/(hr.)(g.)
S	Cyclohexene
T	Absolute temperature, ^oK
W	Water
ΔE_1	Activation energy for rate constant, (k.cal.)/(g.mole)
ΔE_i	Activation energy for adsorption of component i, (k.cal)/(g.mole)

Definitions:

$$RSS = \sum_{i=1}^{n} (r_i - \hat{r}_i)^2$$

$$\sigma^2 = \sum_{i=1}^{n} (r_i - \hat{r}_i)^2 / DF$$

$$\text{Avg.Abs.per cent Error} = \frac{1}{n} \sum_{i=1}^{n} \left[\frac{r_i - \hat{r}_i}{r_i}\right] (100)$$

3.1 INTRODUCTION

The study of the kinetic transformations of coupled heterogeneous catalytic reaction is of practical importance, since most industrial heterogeneous catalytic processes are stoichiometrically complex. From a theoretical point of view the study of the kinetics of coupled systems makes it possible to investigate the mutual influencing of single reactions and the occurrence of some phenomena unknown in the kinetics of complex reactions in the homogeneous phase.

This approach can yield additional information about interactions between the reactants and the surface of the solid catalysts. The kinetic analysis including the effects of products and other addends could also show whether it can provide information about identity or nonidentity of active centres for the parallel dehydrogenation and dehydration of alcohols on oxide catalysts.

Although several investigators [1-4] have made experimental studies on the decomposition of cyclohexanol, the reaction was more complex than had been recognized (Section 2). The decomposition of cyclohexanol leading exclusively either to cyclohexene or to cyclohexanone has frequently been used as a model reaction in studying the mechanism either dehydration or dehydrogenation and in testing the corresponding catalysts [5-6]. A quantitative study of the kinetics and mechanisms of the coupled systems, in general,

where both reactions proceeded as parallel reactions has attracted little attention [7-9].

Emelyanov et al. [1] investigated the effect of carrier and promotor on the properties of copper catalysts in the dehydrogenation of cyclohexanol. The reported activation energy was between 5.5 to 8.6 K.cal/mole. Rovsic et al.[2] presented the structure, activity and selectivity for the industrial copper-magnesium catalyst. The activity and selectivity was determined in a continuous dehydrogenation of cyclohexanol to cyclohexanone between 240-340°C. The yield of cyclohexanone increased upto 290°C and then rapidly decreased (due to phenol formation).

The changes in the structure of a catalyst during catalytic reaction - dehydrogenation of cyclohexanol on NiO were investigated by Ratnaswamy et al. [3]. They inferred that during the reaction the catalyst undergoes reduction to the metallic state.

Pillai and Kuloor [4] studied the dehydrogenation of cyclohexanol in a fixed bed of a catalyst ($Cu:Cr_2O_3:Ni.K_2O:U$) in the temperature range of 210-310°C. The data are expressed in the form of first order forward and second order backward rate expression.

No systematic quantitative analysis of the experimental data on decomposition of cyclohexanol over $NiO-Al_2O_3$ system has been reported. Also values of the rate coefficients and

adsorption coefficients are unknown. Accuracy of the experimental data is of no guarantee of successful kinetic analysis when the experimental programme suffers from lack of insight into the effect of different variables. Froment [10] has discussed in detail the estimation of parameters and has emphasized the necessity of the statistical testing of the results.

In this investigation, increased emphasis has been placed on model discrimination and parameter estimation. The reaction was studied at atmospheric pressure in the temperature range of 300-350°C where the homogeneous reaction was negligible. The experimental results are analysed on the basis of Langmuir-Hinshelwood kinetics with statistical data interpretation to show the real significance of mechanism determination with precise experimental data.

3.2 EXPERIMENTAL

3.2.1 Catalyst Preparation and Characterization:

The preparation of $NiO-Al_2O_3$ catalyst systems along with their characterization by means of X-ray, i.r., d.t.a., t.g.a., electron microscopy and B.E.T. studies have been reported in Section 1. The composition of the catalyst was chosen on the basis of an earlier study(Section 2) where it was established that the activity passed through a maximum over a catalyst composition of about 15 per cent by weight of NiO on alumina calcined at 450°C for 12 hours. The catalytic activity was defined as the number of moles of cyclohexanone formed per unit time per unit weight of the catalyst. All runs described in this study were performed exclusively with the catalyst of this composition (surface area = 87 m^2/g).

3.2.2 Apparatus and Procedure:

The flow system with general experimental procedures and method of analysis have already been described in Section 2. To establish the experimental conditions for which the reaction rate was not influenced by external and internal diffusion, the influence of space velocity, catalyst: mass and particle size was studied as in the usual manner [11]. As a result of these preliminary studies the kinetic measurements were performed at flow rates from 0.57 - 5.7 moles hr^{-1} (N.T.P.). Data were collected at temperatures of 300, 325 and 350°C.

All reaction rate measurements were made after the establishment of steady catalyst activity level. The various compositions of feed for each isothermal set of runs are given in Table 1. In each case an accurate measurement of the rate was possible because at least one of the product was not present in the feed. It is well established that in dehydration water has substantially greater adsorption coefficients than olefin and in dehydrogenation it is ketone which has greater adsorption coefficients than hydrogen [12,13].

Dehydration conversions were calculated from the amount of cyclohexene and dehydrogenation conversions from the amount of cyclohexanone in the reaction products. Other side reactions were not observed to take place under conditions of measurements.

$$\text{Dehydrogenation rate } (r_1) = \frac{\text{Moles of cyclohexanone formed}}{(\text{hr})(\text{gm. of catalyst})}$$

$$\text{Dehydration rate } (r_2) = \frac{\text{Moles of cyclohexene formed}}{(\text{hr})(\text{gm of catalyst})}$$

$$\text{Overall reaction rate}(r_T) = \frac{\text{Moles of cyclohexanol reacted}}{(\text{hr})(\text{gm. of catalyst})}$$

$$(r_T = r_1 + r_2)$$

TABLE 1: EXPERIMENTAL FEED COMPOSITIONS

Run Numbers	Cyclohexanol (mole per cent)	Cyclohexanone (mole per cent)	Water (mole percent)	Nitrogen (mole per cent)
1,18,35	100	-	-	-
2,19,36	10	-	-	90
3,20,37	20	-	-	80
4,21,38	30	-	-	70
5,22,39	40	-	-	60
6,23,40	90	10	-	-
7,24,41	80	20	-	-
8,25,42	70	30	-	-
9,26,43	10	10	-	80
10,27,44	20	10	-	70
11,28,45	30	10	-	60
12,29,46	20	-	80	-
13,30,47	40	-	60	-
14,31,48	60	-	40	-
15,32,49	5	-	10	85
16,33,50	10	-	10	80
17,34,51	15	-	10	75

3.3 RESULTS AND DISCUSSION

The measured reaction rate data are summarized in Table 2. The partial pressures are average of inlet and outlet values. The data points in which the reaction feed was a mixture of cyclohexanol and only one other component are illustrated in Figure 1. This graph indicates that the adsorption of water has appreciable effect on the reaction rate and must be considered in any mathematical rate expression; cyclohexanone has very little effect on the rate.

The treatment of the experimental data is somewhat complicated because of the complex nature of the coupled reaction system and the number of independent variables, that is, the four partial pressures and temperature in each reaction. The techniques of linear and nonlinear estimations were applied to various mathematical rate expressions as a method of correlating the experimental data. Based on Langmuir-Hinshelwood kinetics the models were examined with respect to experimental data using the approach suggested by Hougen and Watson [14]. In this method various mechanisms which might control the reaction are postulated based on single-site and two types of active sites.

3.3.1 Mathematical Modelling Technique:

A nonlinear computer program utilising the Marquardt's algorithm [15, 16] was used to obtain a mathematical fit for

TABLE 2: SUMMARY OF RATE DATA

Run No.	Average Partial Pressure, atm.						Rate, g. moles $hr^{-1} g.^{-1} \times 10^3$		
	Cyclo-hexanol	Cyclo-hexanone	Hydrogen	Cyclo-hexene	Water	Nitrogen	r_T	r_1	r_2
1	2	3	4	5	6	7	8	9	10
				Average Temperature = 300°C					
1	0.9000	0.0162	0.0162	0.0332	0.0332	0.0000	37.5	12.2	25.3
2	0.0989	0.0003	0.0003	0.0007	0.0007	0.8992	6.4	1.8	4.6
3	0.1960	0.0008	0.0008	0.0025	0.0025	0.7973	11.6	2.9	8.7
4	0.2899	0.0023	0.0023	0.0054	0.0054	0.6950	18.1	5.4	12.7
5	0.3828	0.0041	0.0041	0.0080	0.0080	0.5926	21.7	7.2	14.5
6	0.8069	0.1280	0.0134	0.0258	0.0258	0.0000	34.0	11.6	22.4
7	0.7431	0.2049	0.0110	0.0205	0.0205	0.0000	28.9	10.1	18.8
8	0.6565	0.3019	0.0088	0.0164	0.0164	0.0000	26.0	9.0	17.0
9	0.0992	0.1001	0.0002	0.0005	0.0005	0.7994	5.1	1.4	3.7
10	0.1968	0.1006	0.0008	0.0019	0.0019	0.6981	9.4	2.9	6.5
11	0.2915	0.1025	0.0028	0.0044	0.0044	0.5945	16.6	6.5	10.1
12	0.1966	0.0005	0.0005	0.0023	0.8005	0.0000	9.8	1.8	8.0
13	0.3879	0.0021	0.0021	0.0066	0.6014	0.0000	15.2	3.6	11.6
14	0.5711	0.0042	0.0042	0.0131	0.4074	0.0000	20.6	5.1	15.5
15	0.0497	0.0001	0.0001	0.0002	0.1002	0.8498	3.6	1.1	2.5
16	0.0994	0.0002	0.0002	0.0004	0.1003	0.7996	4.0	1.1	2.9
17	0.1479	0.0003	0.0003	0.0009	0.1013	0.7490	6.0	1.4	4.6
				Average Temperature = 325°C					
18	0.8700	0.0229	0.0229	0.0421	0.0421	0.0000	51.3	18.1	33.2
19	0.0983	0.0005	0.0005	0.0009	0.0009	0.8986	10.5	3.6	6.9
20	0.1945	0.0016	0.0016	0.0029	0.0029	0.7964	15.8	5.8	10.0
21	0.2868	0.0042	0.0042	0.0060	0.0060	0.6928	23.8	9.8	14.0

Table 2 (cont'd)

1	2	3	4	5	6	7	8	9	10
22	0.3750	0.0067	0.0067	0.0112	0.0112	0.5893	31.8	11.9	19.9
23	0.7840	0.1320	0.0190	0.0324	0.0324	0.0000	45.9	17.0	28.9
24	0.7200	0.2085	0.0175	0.0272	0.0272	0.0000	41.9	16.3	25.6
25	0.6406	0.3043	0.0140	0.0205	0.0205	0.0000	36.5	14.8	21.7
26	0.0985	0.1007	0.0005	0.0009	0.0009	0.7986	9.4	3.3	6.1
27	0.1944	0.1011	0.0019	0.0026	0.0026	0.6980	13.7	4.7	9.0
28	0.2899	0.1025	0.0029	0.0054	0.0054	0.5937	19.5	6.9	12.6
29	0.1958	0.0009	0.0009	0.0027	0.7997	0.0000	12.3	2.9	9.4
30	0.3842	0.0029	0.0029	0.0084	0.6017	0.0000	19.9	5.1	14.8
31	0.5637	0.0057	0.0057	0.0162	0.4087	0.0000	26.4	6.9	19.5
32	0.0497	0.0001	0.0001	0.0003	0.1003	0.8499	5.1	1.5	3.6
33	0.0989	0.0003	0.0003	0.0007	0.1006	0.7922	6.9	2.2	4.7
34	0.1475	0.0007	0.0007	0.0015	0.1018	0.7480	9.8	2.9	6.9
				Average Temperature = 350°C					
35	0.8467	0.0303	0.0303	0.0464	0.0464	0.0000	62.2	24.6	37.6
36	0.0974	0.0009	0.0009	0.0015	0.0015	0.8979	16.4	5.8	10.6
37	0.1917	0.0028	0.0028	0.0042	0.0042	0.7944	24.3	9.8	14.5
38	0.2825	0.0055	0.0055	0.0079	0.0079	0.6905	31.8	13.3	18.8
39	0.3685	0.0094	0.0094	0.0130	0.0130	0.5865	40.5	17.0	23.5
40	0.7661	0.1362	0.0246	0.0365	0.0365	0.0000	55.7	22.4	33.3
41	0.7044	0.2118	0.0222	0.0308	0.0308	0.0000	51.0	21.3	29.7
42	0.6247	0.3066	0.0191	0.0248	0.0248	0.0000	47.4	20.6	26.8
43	0.0977	0.1006	0.0008	0.0013	0.0013	0.7983	14.5	5.4	9.1
44	0.1930	0.1016	0.0022	0.0037	0.0037	0.6959	20.2	7.6	12.6
45	0.2866	0.1036	0.0043	0.0067	0.0067	0.5922	25.7	10.1	15.6
46	0.1940	0.0012	0.0012	0.0037	0.8000	0.0000	17.3	4.3	13.0
47	0.3822	0.0033	0.0033	0.0095	0.6018	0.0000	22.4	5.8	16.6
48	0.5614	0.0063	0.0063	0.0171	0.4089	0.0000	28.2	7.6	20.6
49	0.0494	0.0002	0.0002	0.0004	0.1004	0.8495	7.9	2.5	5.4
50	0.0985	0.0005	0.0005	0.0010	0.1008	0.7989	9.8	3.3	6.5
51	0.1464	0.0010	0.0010	0.0022	0.1022	0.7473	14.1	4.7	9.4

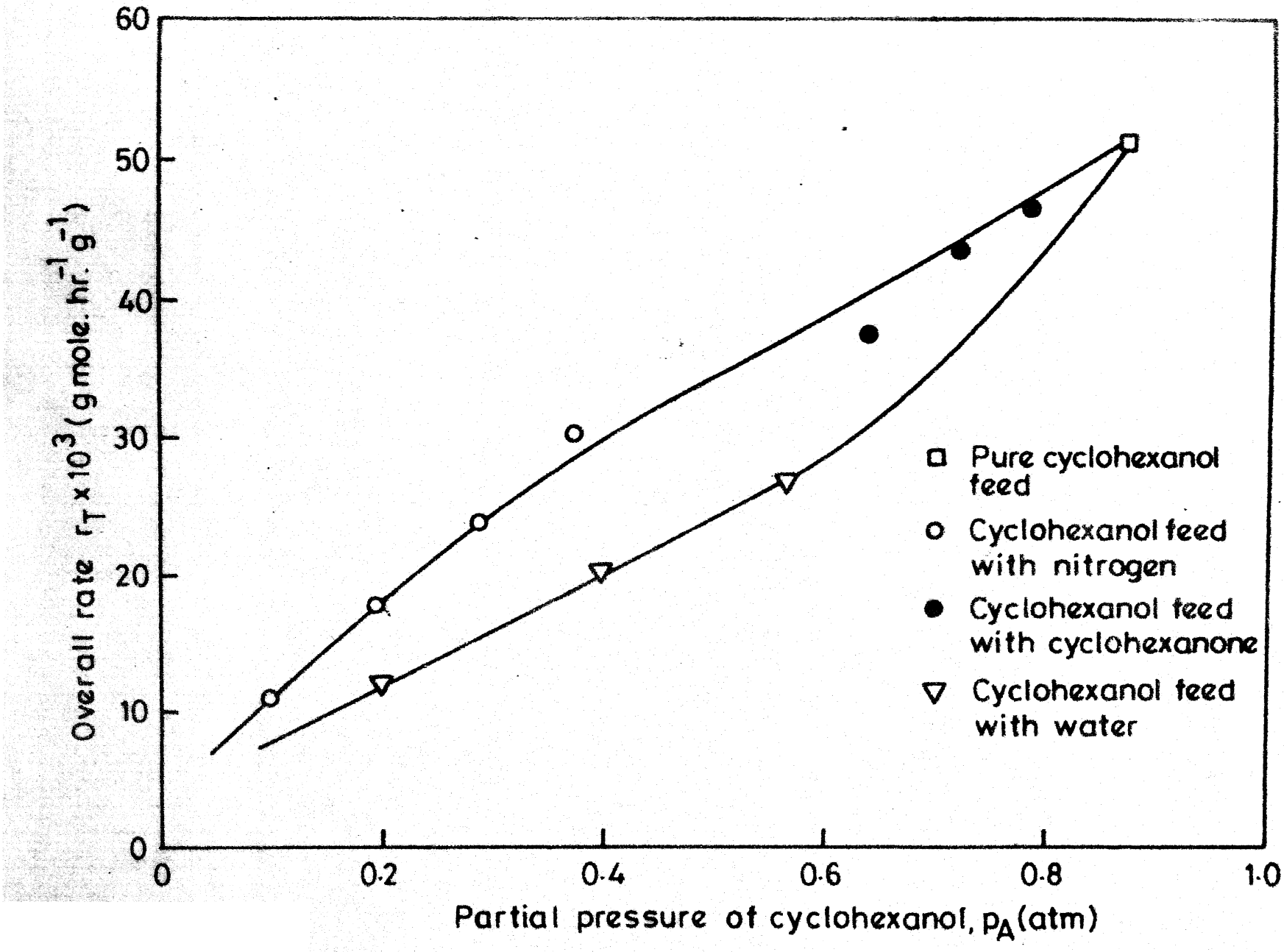

Fig. 1 - Partial rate data at 325 °C.

various Hougen and Watson types of rate equations [17]. This program minimised the residual sum of squares (RSS) during the regression. The nonlinear computer program improved basically upon the initial estimates of the various constants of the rate equation until the RSS could no longer be reduced. Approximate 95 per cent confidence intervals for the various constants were calculated from estimates of their individual variances, (σ^2).

3.3.2 Model Comparison:

An estimate of the variance of each model was calculated from the RSS and the appropriate degrees of freedom (DF). The various models were compared statistically by forming a variance ratio. An F test with the proper degrees of freedom was then used to determine if the variances were significantly different at the 95 per cent level [18]. Models can be rejected on the basis of negative adsorption constants or improper trends of these constants with the temperature when, in actuality, these constants are positive or have negative temperature coefficients. Of course, physical mechanisms which have such properties as adsorption constants with positive temperature coefficients are extremely rare and if the constants of a model are actually unacceptable, the model has generally been rejected [19].

3.3.3 Data Analysis:

The coupled reaction system studied has the following reaction scheme

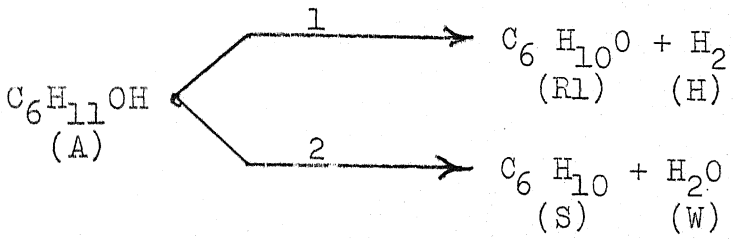

The possible isothermal rate equations for dehydrogenation based on single and dual-site mechanisms with the assumption of an irreversible reaction are presented in Table 3. Similar rate expressions were used for dehydration rate data (subscripts R1 and H were replaced by S and W, respectively). These rate equations were derived with an adsorption term for each of the reaction components and diluent nitrogen. Linear and nonlinear regressions of the rate equations were made at each temperature. All possible combinations of the various adsorption terms were examined in order to allow for various negligible adsorption terms. The isothermal rate equations, basic types of which are given in Table 3, thus resulted in twenty-four different mathematical forms. The method of Yang and Hougen [17] was used to eliminate some of the rate controlling steps. The rate data showed that the desorption of product was not a rate controlling step. Rate expressions were eliminated from further

TABLE 3: POSSIBLE ISOTHERMAL RATE EQUATIONS

Reaction $C_6H_{11}OH$ (A)

1 → $C_6H_{10}O$ (Rl) + H_2 (H)

2 → C_6H_{10} (S) + H_2O (W)

Inert: Nitrogen (N)

A. Single-Site Mechanism

Rate Controlling Step	Rate Equation
a. Adsorption of cyclohexanol A	$K_1 K_A p_A/(1+K_{Rl} p_{Rl}+K_H p_H+K_N p_N)$
b. Surface reaction	$K_1 K_A p_A/(1+K_A p_A+K_{Rl} p_{Rl}+K_H p_H+K_N p_N)$
c. Desorption of cyclohexanone Rl	K_1
d. Desorption of Hydrogen H	K_1

B. Dual-Site Mechanism

Rate Controlling Step	Rate Equation
a. Adsorption of Cyclohexanol A	$K_1 K_A p_A/(1+K_{Rl} p_{Rl}+K_H p_H+K_N p_N)$
b. Surface reaction	$K_1 K_A p_A/(1+K_A p_A+K_{Rl} p_{Rl}+K_H p_H+K_N p_N)^2$
c. Desorption of cyclohexanone Rl	K_1
d. Desorption of Hydrogen H	K_1

consideration when any of the converged adsorption constants became negative.

Table 4 gives the rate models with all positive constants which had to be retained statistically after the isothermal regressions. The converged values of the parameters of these models both by linear and nonlinear estimations are presented in Table 5.

The data were most satisfactorily correlated by Model D14 (dual-site surface reaction with cyclohexanol adsorbed) for dehydrogenation while the kinetics of dehydration on this catalyst could be better described by Model D13(dual-site surface reaction with cyclohexene not adsorbed).

The effect of temperature on the rate expressions was introduced by substituting the Arrhenius temperature dependency relation for each of the parameters:

$$K_1 = K_1^o \, e^{-\Delta E_1/RT}$$

The model D14 for dehydrogenation then becomes

$$r_1 = \frac{K_1^o \, e^{-\Delta E_1/RT} \; K_A^o \, e^{-\Delta E_A/RT} \; p_A}{(1 + K_A^o \, e^{-\Delta E_A/RT} \, p_A)^2}$$

Similarly, for dehydration the model D13 becomes

$$r_2 = \frac{K_1^o \, e^{-\Delta E_1/RT} \; K_A^o \, e^{-\Delta E_A/RT} \; p_A}{(1+K_A^o \, e^{-\Delta E_A/RT} \, p_A + K_W^o \, e^{-\Delta E_W/RT} \, p_W)^2}$$

The converged values of the parameters of these expressions

TABLE 4: MODELS REMAINING AFTER ISOTHERMAL REGRESSION

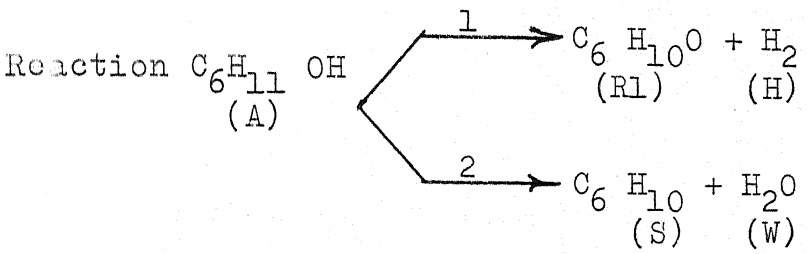

Model	Rate Controlling Step	Rate Equation: Dehydrogenation	Rate Equation: Dehydration
S13	Single-site surface reaction with cyclohexene(S) not adsorbed	-	$\frac{K_1 K_A p_A}{(1+K_A p_A+K_W p_W)}$
S14	Single-site surface reaction with cyclohexanol(A) adsorbed	$\frac{K_1 K_A p_A}{(1+K_A p_A)}$	$\frac{K_1 K_A p_A}{(1+K_A p_A)}$
D13	Dual-site surface reaction with cyclohexene(S)not adsorbed	-	$\frac{K_1 K_A p_A}{(1+K_A p_A+K_W p_W)^2}$
D14	Dual-site surface reaction with cyclohexanol(A)adsorbed	$\frac{K_1 K_A p_A}{(1+K_A p_A)^2}$	$\frac{K_1 K_A p_A}{(1+K_A p_A)^2}$

TABLE 5: ISOTHERMAL REGRESSION

Model	Temp., (°C)	$K_1 \times 10^3$ (g.moles $hr^{-1} g^{-1}$) Linear	$K_1 \times 10^3$ (g.moles $hr^{-1} g^{-1}$) Non-Linear	K_A (atm^{-1}) Linear	K_A (atm^{-1}) Non-linear	K_V (atm^{-1}) Linear	K_V (atm^{-1}) Nonlinear	Avg. Abs. per cent Error Linear	Avg. Abs. per cent Error Non-linear	RSS Linear	RSS Non-linear
				Dehydrogenation							
S14	300	118.7	117.6±2.0	0.1175	0.125±0.27			15.2	5.78	0.60×10^{3}	0.3749×10^{-4}
	325	56.0	106.0±4.0	0.4530	0.232±0.34			2.4	3.30	0.36×10^{3}	0.1132×10^{-3}
	350	42.0	206.3±7.0	0.9860	0.424±0.40			0.34	4.70	0.86×10^{2}	0.3159×10^{-3}
N14	300	98.9	81.7±4.4	0.4340	0.2045±0.16			0.02	3.60	0.42×10^{1}	0.3873×10^{-4}
	325	119.3	231.8±4.7	0.2190	0.1057±0.15			0.15	3.04	0.21×10^{1}	0.1134×10^{-3}
	350	203.0	759.1±8.0	0.0710	0.0382±0.35			8.10	3.90	0.47×10^{1}	0.3171×10^{-3}
				Dehydration							
S13	300	52.3	57.0±4.0	0.8698	0.80 ±0.20	1.2156	0.3±0.8	1.60	2.50	0.12×10^{4}	0.4305×10^{-4}
	325	63.5	77.0±5.0	0.9700	0.75 ±0.13	0.0800	0.37±0.9	6.00	3.60	0.27×10^{3}	0.761×10^{-4}
	350	55.0	60.0±9.0	1.7500	1.47 ±0.40	0.5110	0.83±0.3	8.40	5.00	0.37×10^{3}	0.140×10^{-3}
S14	300	43.4	58.3±3.0	1.3480	0.72 ±0.16			7.50	1.20	0.30×10^{3}	0.4824×10^{-3}
	325	65.0	85.6±10.0	0.9215	0.6284±0.34			14.00	3.30	0.26×10^{3}	0.7844×10^{-4}
	350	54.5	64.8±8.0	1.6640	1.25 ±0.33			7.50	2.90	0.31×10^{3}	0.1823×10^{-3}
N13	300	140.0	107.0±4.0	0.6600	0.4137±0.08	0.2000	0.4420±0.31	0.17	2.12	0.62×10^{1}	0.434×10^{-4}
	325	146.0	167.0±5.0	0.4200	0.3587±0.04	0.0500	0.3213±0.16	1.10	2.80	0.31×10^{1}	0.784×10^{-4}
	350	164.0	258.0±9.0	0.3100	0.2967±0.13	0.0200	0.3068±0.25	0.41	3.50	0.54×10^{1}	0.148×10^{-2}
N14	300	118.0	141.4±3.0	0.4600	0.2900±0.06			0.19	0.80	0.47×10^{1}	0.4964×10^{-4}
	325	149.0	200.0±4.0	0.4100	0.2600±0.07			1.02	1.60	0.31×10^{1}	0.8077×10^{-4}
	350	135.0	166.7±6.0	0.6500	0.4500±0.09			0.40	4.20	0.53×10^{1}	0.1947×10^{-3}

are given in Table 6. The values of activation energies for the adsorption term are negative indicating a satisfactory temperature relationship. The E_1 is positive as would be expected.

The apparent activation energies for dehydrogenation and dehydration are 28.6 and 12.4 kcal $mole^{-1}$, respectively, in agreement with the values reported by Viswanathan and Yaddanapalli [20]. This indicates that one of the effects of NiO on Al_2O_3 may be the physical coverage of the surface resulting in the loss of surface of the dehydration of cyclohexanol and promotion of a competitive dehydrogenation reaction.

The results of this work indicate that dehydrogenation and dehydration proceed on different sites of the catalyst. Nevertheless, comparable values of adsorption coefficients of cyclohexanol for these two reactions show that primary interaction of the cyclohexanol is rather non-specific; it might take place on surface sites which are not identical with reaction centres participating in further transformation of adsorbed cyclohexanol. This primary interaction could be of physical character [8,9]; physical character of the adsorption of the reaction components is atleast partially indicated also by the fact that the gaseous component (hydrogen) does not influence the reaction, while other (water) does.

TABLE 6: CONVERGED VALUES OF THE PARAMETERS

Parameter	Estimate
D14-Dehydrogenation	
K_1^o	5.35×10^9
ΔE_1	28.66 kcal(g.mole^{-1})
K_A^o	2.8×10^{-8}
ΔE_A	-17.89 kcal(g.mole^{-1})
D13-Dehydration	
K_1^o	4.5×10^3
ΔE_1	12.4 kcal(g.mole^{-1})
K_A^o	1.3×10^{-2}
ΔE_A	-3.87 kcal(g.mole^{-1})
K_W^o	8.7×10^{-4}
ΔE_W	-8.91 kcal(g.mole^{-1})

This assumption could explain why water retards the reaction by which it is formed. Though the best dehydrogenation mechanism arrived by statistical analysis is independent of cyclohexanone adsorption coefficient, physically it does show little effect (Figure 1). This may be the case where water adsorbs on dehydrogenation active centres, on which the reaction which would lead to cyclohexanone formation does not take place at all.

3.4 CONCLUSIONS AND RECOMMENDATIONS

Results on the decomposition of cyclohexanol over $NiO-Al_2O_3$ show that water affects significantly the dehydration rate and this effect of product adsorption must be included in the mechanism. For dehydrogenation, the data were most satisfactorily correlated by a mechanism of dual-site surface reaction which assumes that the rate controlling step was the adsorption of cyclohexanol. Similarly, the kinetics of dehydration was described by a dual-site surface reaction with cyclohexene not adsorbed. The apparent activation energies for dehydrogenation and dehydration are 28.6 and 12.4 k cal $mole^{-1}$, respectively.

It is expected that the present result will contribute to the understanding of the kinetics and mechanisms of the coupled reaction systems.

Although, the proposed models for the dehydrogenation and dehydration satisfactorily explained the kinetic data, the assumptions which are made in the development of the particular rate expression must be verified individually.

REFERENCES

1. Emelyanov, N.P., Belskaya, R.I., and Taborisskaya, E.A., Vestsi Akad. Navuk Belarus, SSR, Ser. Khim. Navuk. 1, 103 (1972).
2. Rovsii, V.A., Belskaya, R.I., and Zaretskii, M.V., Vestsi Akad. Navuk Belarus, SSR, Ser. Khim. Navuk. 1, 24 (1973).
3. Ratnaswamy, A.V., Yeddanapalli, P., and Lourelu, M., Curr. Sci. 39, 316 (1970).
4. Pillai, T.J.R., and Kuloor, N.R., Ind. J.Tech. 12, 327 (1974).
5. Morita, H., Kawashima, E., and Nomura, K., Kanazawa Daijaku. Kogakubu. Keyo (Japan) 5, 389 (1970).
6. Kuriacose, J.C., Daniel, C., and Swaminathan, R., J.Catal. 12, 19 (1968).
7. Klissurski, D.G., McCaffray, E.F., and Ross, R.A., Can. J.Chem. 49, 3778 (1971).
8. Jamboor, J., and Beranek, L., Coll.Czech. Chem. Comm. 40, 1374 (1975).
9. Beranek, L., Adv. Catalysis. 24, 1 (1975).
10. Froment, G.F., A.I.Ch.E. J. 21, 1041 (1975).
11. Ross, R.A., and Walsh, B.G., J.Appl. Chem. 11, 469 (1961)
12. Balandin, A.A., Konenko, I.R., and Tolstopyatova, A.A., Kinet. Kataliz. 2, 900 (1961).
13. Tolstopyatova, A.A., Balandin, A.A., and Chi-Ch-Uan. Yu, Zh. Fiz. Chem. 37, 2220 (1963).

14. Hougen, O.A., and Watson, K.M., 'Chemical Process Principles. Part III', John Wiley Inc. New York (1947).

15. Marquardt, D.W., J. Soc. Indus. Appl. Math. 11, 431 (1963).

16. Drapper, N.R., and Smith, H., 'Applied Regression Analysis', John Wiley, New York (1966).

17. Yang, K.H., and Hougen, O.A., Chem.Eng. Prog. 46, 146 (1950).

18. Dunn,O.J., and Clark,V.A., 'Applied Statistics', John Wiley, New York (1974).

19. Kittrell,J.R., Hunter, W.G., and Watson, C.C., AIChEJ. 11, 1051 (1965).

20 Viswanathan, V.N., and Yeddanapalli, P., Z. Anorg. Alleg. Chem. 407, 98 (1974).

SECTION 4

KINETICS OF LIQUID PHASE OXIDATION OF TETRALIN OVER NiO-Al_2O_3 SYSTEMS

CONTENTS

LIST OF FIGURES

LIST OF TABLES

4.1 INTRODUCTION

The liquid phase oxidationof tetralin (1,2,3,4 tetrahydronaphthalene) with soluble catalysts have been studied extensively. The work reported so far on insoluble catalysts for the oxidation of tetralin is limited.

George [1] conducted experiments on the surface catalysed oxidation of tetralin with 'inert powders' as catalysts. These inert powders contained very small amounts of transition element impurities. The primary product of the surface catalysed oxidation with the transition element is the hydroperoxide. The effect of tetralin concentration on the rate was studied. The chain termination step involving oxygen was present.

Initiation

$$S + O_2 \xrightarrow{k_1} S..... O_2 \quad \text{(slow)}$$

$$S.....O_2 + RH \xrightarrow{k_2} S + R^{\cdot} + O_2H^{\cdot}$$

Propagation

$$R^{\cdot} + O_2 \xrightarrow{k_3} R\dot{O}_2$$

$$RO_2^{\cdot} + RH \xrightarrow{k_4} RO_2H + R^{\cdot}$$

Termination

$$RO_2^{\cdot} + O_2 \xrightarrow{k_5} RO^{\cdot} + O_3$$

Mukherjee and Graydon [2] studied the liquid phase oxidation of tetralin with insoluble catalysts and the reaction rates have been compared with those of the soluble ones. It was found that the catalysts like oxides of nickel, manganese and copper were extremely active while others like oxides of aluminum and zinc were inactive. The initial product of reaction was found to be tetralin hydroperoxide which decomposed further into its corresponding alcohol and ketone. Kinetic studies have been made with four of the best catalysts and the reaction mechanism was proposed.

Initiation

$$ROOH^{\cdot}M \xrightarrow{k_1} RO^{\cdot}M + OH^{\cdot}M$$

$$RO^{\cdot}M + RH \xrightarrow{k_2} ROH + R^{\cdot}$$

$$^{\cdot}OH\ M + RH \xrightarrow{k_3} H_2O + R^{\cdot}$$

Propagation

$$R^{\cdot} + O_2 \xrightarrow{k_4} RO_2^{\cdot}$$

$$RO_2^{\cdot} + RH \xrightarrow{k_5} ROOH + R^{\cdot}$$

Termination (monomolecular)

$$RO_2^{\cdot} \xrightarrow{k_6} R''\,CO + O_2 + H_2O$$

$$RO_2^{\cdot} \xrightarrow{k_7} R''\,CO + M^{\cdot}OH$$

with R = $C_{10}H_{11}$

M = active site of the catalyst surface

Agarwal and Srivastava [3] studied the kinetics and catalytic behaviour of NiO supported on alumina, activated carbon and $NiMnO_4$ supported on alumina in the liquid phase oxidation of cumene. It was observed that the use of activated carbon as a support instead of alumina induced increased activity, lower activation energies and shifted the limiting oxidation rate to a lower catalyst amount.

It has been established that, for the heterogeneous liquid phase oxidation of tetralin catalysed by transition metal oxides, there is a critical weight of catalyst above which the rate of oxidation drops [2,4-6] which suggested that the rates of formation and distruction of hydroperoxide became equal [7].

George and Robertson [8] have conducted experiments on the liquid phase oxidation of tetralin in the presence of heavy metal catalysts like ferric stearate and copper stearate. It has been shown that the primary reaction is the Chain formation of hydroperoxide in which the catalyst both starts and stops the reaction chains. The subsequent reaction is the unimolecular decomposition of the hydroperoxide to give the ketone. They proposed the following mechanism:

Initiation

$$M + O_2 \xrightarrow{k_1} M.....O_2$$

$$M...O_2 + RH \xrightarrow{k_2} M + R^{\cdot} + O_2H^{\cdot}$$

Propagation

$$R^{\cdot} + O_2 \xrightarrow{k_3} RO_2^{\cdot}$$

$$RO_2^{\cdot} + RH \xrightarrow{k_4} RO_2H + R^{\cdot}$$

Termination

$$RO_2^{\cdot} + O_2 \xrightarrow{k_5} RO^{\cdot} + O_3$$

$$RO_2^{\cdot} + M \xrightarrow{k_6} M....RO_2^{\cdot}$$

Arthur and Robert [9] investigated the kinetics of oxidation of tetralin reactions isothermally and by a heavy metal activation cobaltous-acetate and benzoylperoxide. The rates of isothermal oxidation in the temperature range of 69° - 120°C are slower than the maximum rates observed by other means. This is due to the formation of self inhibitor (r-O-hydroxy phenyl butyric acid) which has been isolated in small amounts from thermally oxidised tetralin.

Recently Srivastava and co-workers [10,11] studied the oxidation of tetralin in the region where inhibition was effective, in the presence of MnO_2 catalyst. Their results favoured the view that this oxidation involved simultaneous formation and distruction of hydroperoxide.

The kinetics and catalytic behaviour of oxidation of tetralin in the presence of supported nickel oxide have not been discussed in the literature although it is well

documented that the activity of a catalyst can be drastically altered by the support used and its method of preparation. Careful attention has been given to the influence of catalyst ratio, catalyst composition, catalyst calcination period and hydrocarbon concentration on the reaction rate in the liquid phase oxidation of tetralin.

4.2 EXPERIMENTAL

4.2.1 Materials

Pure tetralin was obtained from Koch-Light Laboratories Ltd., Monochlorobenzene of Sarabhai M. Chemicals was used as an inert solvent for varying the concentration of tetralin. Oxygen was supplied by Indian Oxygen Limited, Kanpur.

Nickel nitrate hexahydrate was obtained from Robert Johnson and aluminum oxide from Sarabhai M.Chemicals.

Hydroperoxide of tetralin was prepared separately by the oxidation at 60°C using the laboratory prepared $NiO-Al_2O_3$ catalysts.

4.2.2 Catalyst Preparation

The preparation of supported NiO catalysts containing upto 20 weight per cent NiO calcined at 450°C for 4,8 and 12 hours and their characterization along with details of measurements of particle size distribution and crystal growth have been described in Section 1. Reference to various samples will be made as discussed in Section 1.

4.2.3 Apparatus and procedure

A schematic diagram of the experimental set-up for the liquid phase oxidation of tetralin is given in Figure 1.

The reactor consisted of a B55/54 glass joint of capacity 400 cc. Tetralin was purified by the method given by George et al. [8]. The water bath was switched on and allowed to reach the desired steady-state temperature which

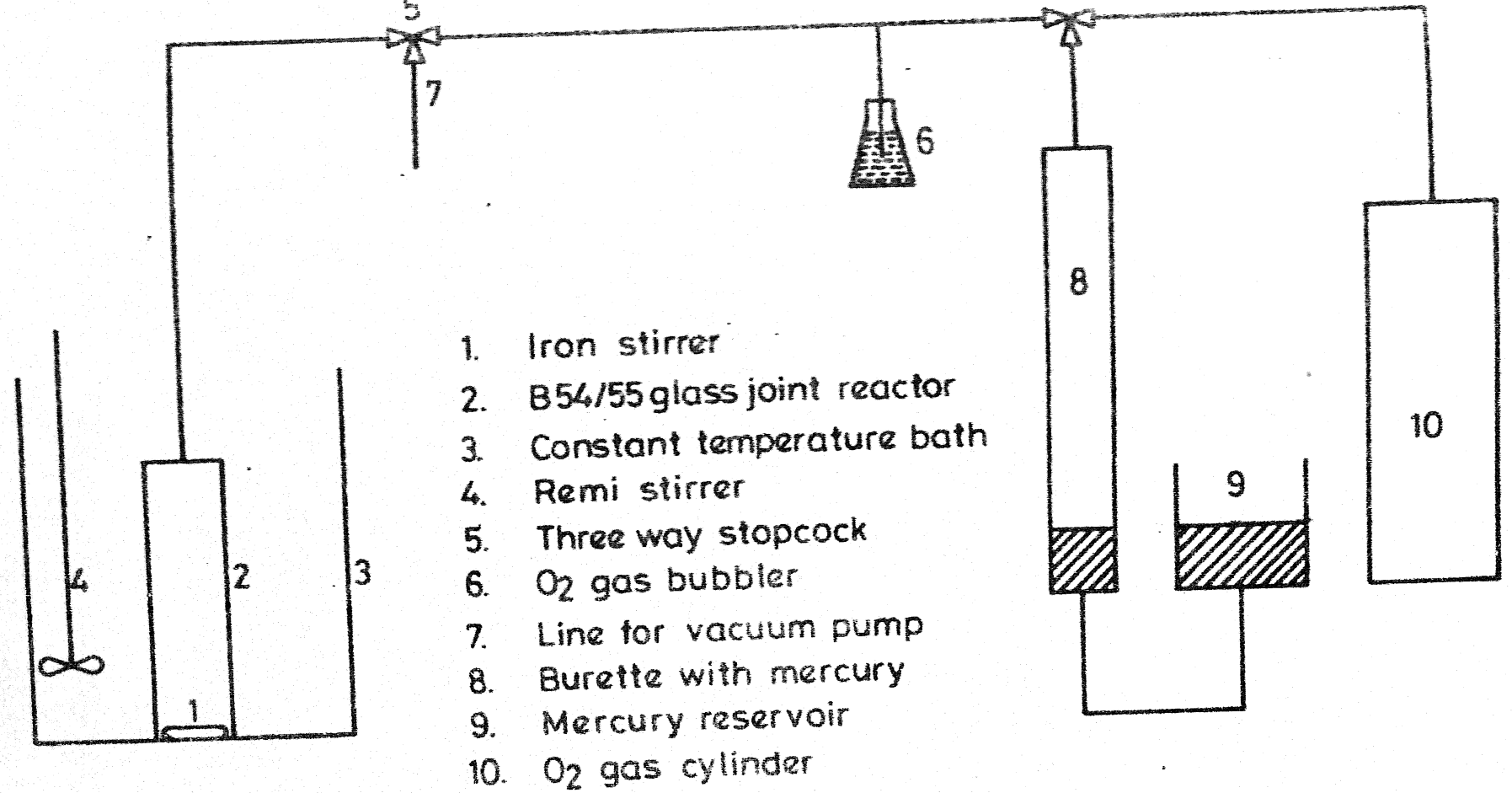

Fig. 1 - Schematic diagram of the experimental set-up.

normally took half an hour. The reactor was well washed and dried. The desired catalyst amount was taken into the reactor and the iron stirring piece was dropped inside the reactor. 20 ml of tetralin was added to the reactor. Little amount of hydroperoxide of known concentration was added to the reactant. The reactor was connected to the burette and the system was evacuated by means of vacuum pump. Then the system was filled with oxygen. The reactor was then placed in the water bath soon after the water bath attained the steady temperature. 15 minutes later the magnetic stirrer was switched on and the change in the burette reading for every five minute interval was recorded. The normal run was taken for 30 minutes after that products were allowed to cool down to room temperature and then centrifuged for 30 minutes at 800 RPM in order to separate the catalyst particles from the reaction products. The reaction products were hydroperoxide, tetraol, and tetralone as were analysed by Mukherjee et al.[2].

4.2.4 Iodometric method

In a 250 ml flask 40 ml of isopropyl alcohol, 2 ml of acetic acid and the sample (5 ml) were taken and heated to reflux. Then 10 ml of saturated solution of sodium iodide in isopropyl alchol at room temperature (prepared by refluxing 25 gms of sodium iodide with 100 ml of isopropyl alcohol) was added to the flask and refluxed for 5 minutes. 5 ml of water was added and titrated with 0.1N $Na_2S_2O_3$ to the

disappearance of yellow color. This was used to analyse the concentration of peroxide present in tetralin and added peroxide to start up the reaction.

4.3 RESULTS AND DISCUSSION

The symbols RH, ROOH and ROH are used in general for hydrocarbon, hydroperoxide and alcohols respectively. Catalyst weight to hydrocarbon ratio is defined as the weight of the catalyst in grams divided by the volume of tetralin in ml.

From the earlier experiments [2] it was concluded that addition of both catalyst and hydroperoxide was necessary to initiate the oxidation of tetralin. This was evident in the present study. A critical ratio of hydroperoxide concentration to catalyst amount of approximately 3-4 x 10^{-4} g.mole/g of catalyst was obtained. Further runs were conducted with this ratio.

4.3.1 Effect of NiO Concentration

Figure 2 shows the rate of oxygen absorption as a function of weight per cent of NiO for different calcination periods. In the cases of 4 and 8 hours periods of calcination, the rates declined after 10 per cent by weight of NiO concentration, however, for the 12 hours calcination period the rates continuously increased with increase in concentration of NiO.

The color of the catalysts varied from green, greyish green to black as the weight percent of NiO increased in the catalyst samples as well as with duration of calcination. The samples of 12 hours calcination are black in color. The black, grey and green forms of NiO were studied by X-ray method which showed a greater broadening of the diffraction

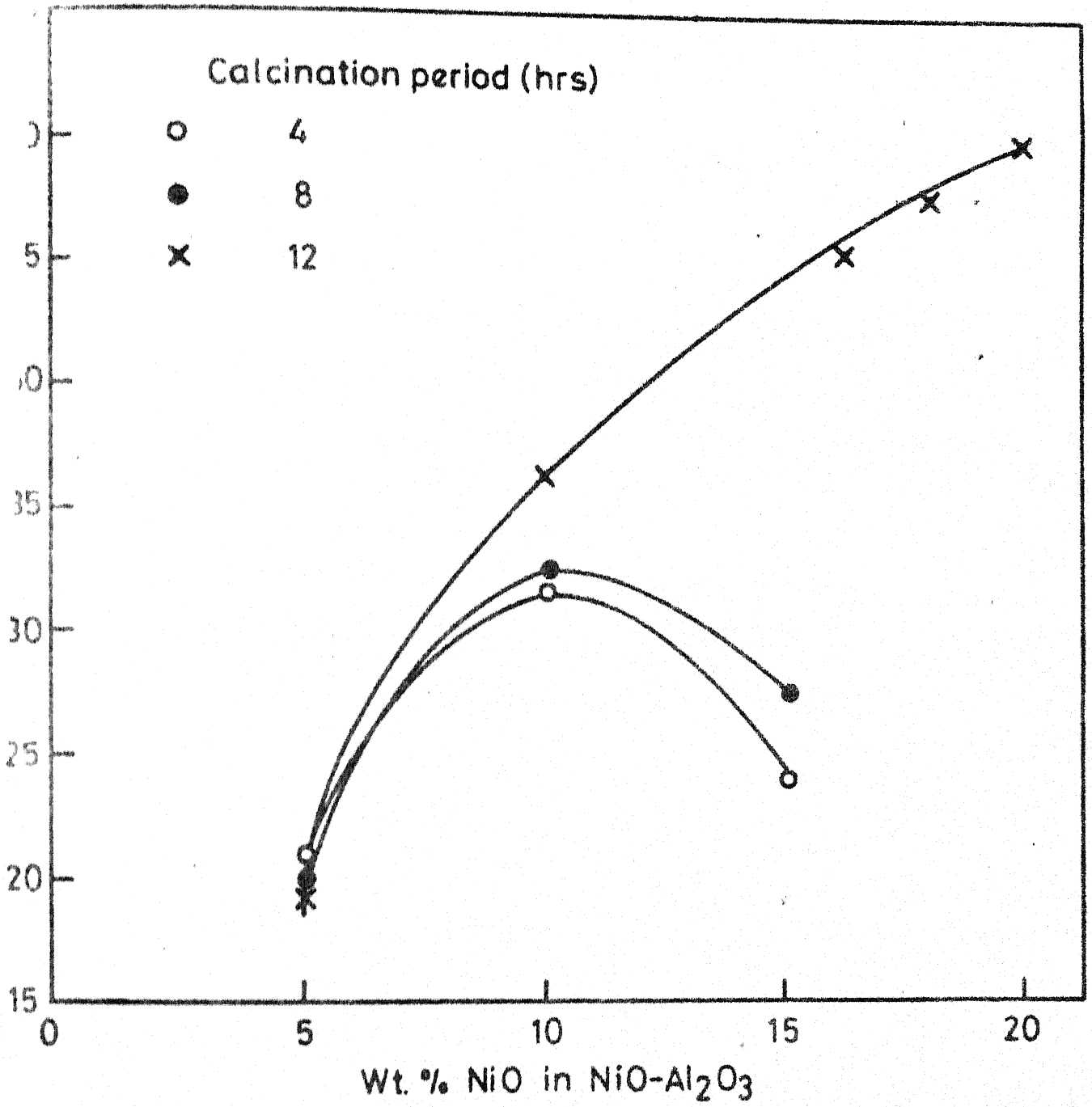

Fig. 2 - The dependence of oxygen absorption rate on the weight percent of NiO for tetralin oxidation at 65°C and at a catalyst ratio of 0.25 gm/ml.

lines of the black form over these of grey and green forms. The color variation may be due to lattice imperfections attributed to excess oxygen and the green form is the stoichiometric oxide. The black color of the catalyst indicates the presence of stoichiometrically excess oxygen in the lattice of NiO and increases with the p-type semiconductivity of NiO. This could account for increase in activity [12-14]. In the cases of 4 and 8 hours calcination, there appeared to be occluded oxides of nitrogen in the impregnated samples thus accounting for the decrease in rate after 10 per cent by weight of NiO in the catalyst samples. The increase in rate in all the samples calcined at 12 hours may be due to the removal of occluded gases by prolonged heating [15]. Since 20 per cent NiO supported on Al_2O_3 catalyst calcined for 12 hours gave the maximum rate of all the rates, further experiments were performed with this catalyst. The surface area (S_A), pore volume (V_P) and porosity of the samples together with the calculated value of pore radii ($\bar{r} = 2V_P/S_A$) are given in Table 1 of section 1.

Figures 3 gives the comparison of rates of oxygen absorption versus catalyst ratio for 20 per cent NiO on Al_2O_3 and pure NiO. It may be seen that the rate with 20 per cent $NiO-Al_2O_3$ catalyst is higher than that of pure NiO. Immediately apparent from the rate plots of Figure 3 is an observable effect; the oxidation increased with increased catalyst ratios and

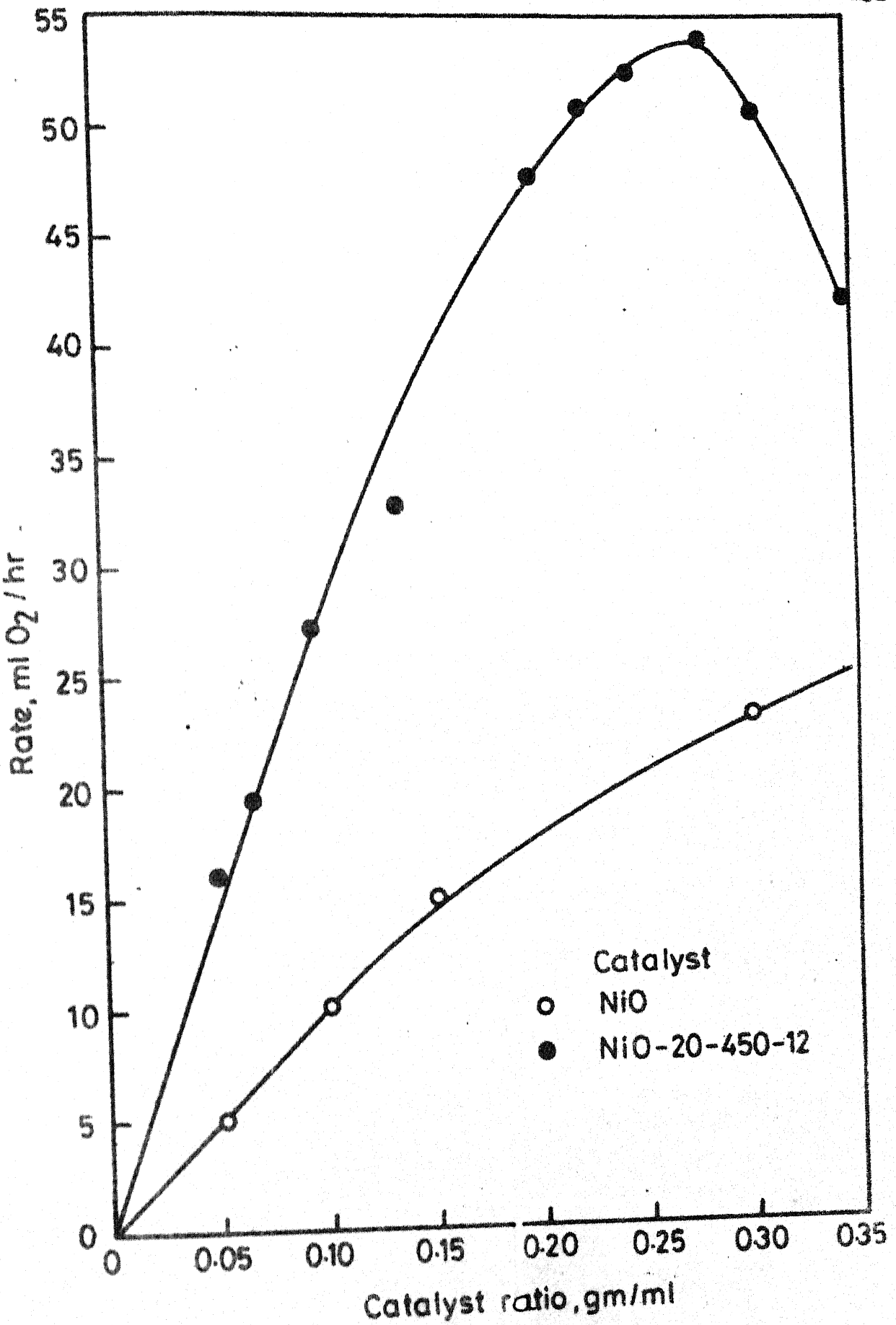

Fig. 3 - The dependence of oxygen absorption rate

reached a maximum at 0.28 gm/ml. A further increase in the catalyst ratio resulted in the decrease of the rate. The decrease in rate after the maximum was also observed by Mukherjee et al. [2].

4.3.2 Influence of Hydrocarbon Concentration-Catalyst Weight and Temperature of Reaction

The influence of hydrocarbon concentration on the rate of oxidation of tetralin was studied with the mixtures of tetralin and monochlorobenzene. Runs were made at the catalyst ratio of 0.10 gm/ml. The ratio was chosen on the basis that in this region of catalyst ratio, the limiting rate of oxidation was not attained. The order with respect to hydrocarbon concentration was 1.0.(Figure 4.) A plot of rate of oxygen consumption versus the hydrocarbon concentration at a catalyst ratio where the limiting oxidation is reached, is also given in Figure 4. An order of 2 was found with respect to hydrocarbon concentration.

In order to improve confidence in the reported orders, runs were also made at catalyst ratios near to levels at which the kinetic regime was considered unstable. Included in Figure 4 is a plot of rate against hydrocarbon concentration for a catalyst ratio of 0.2 gm/ml. The apparent order of 1.3 possibly results from transition between these more normal responses.

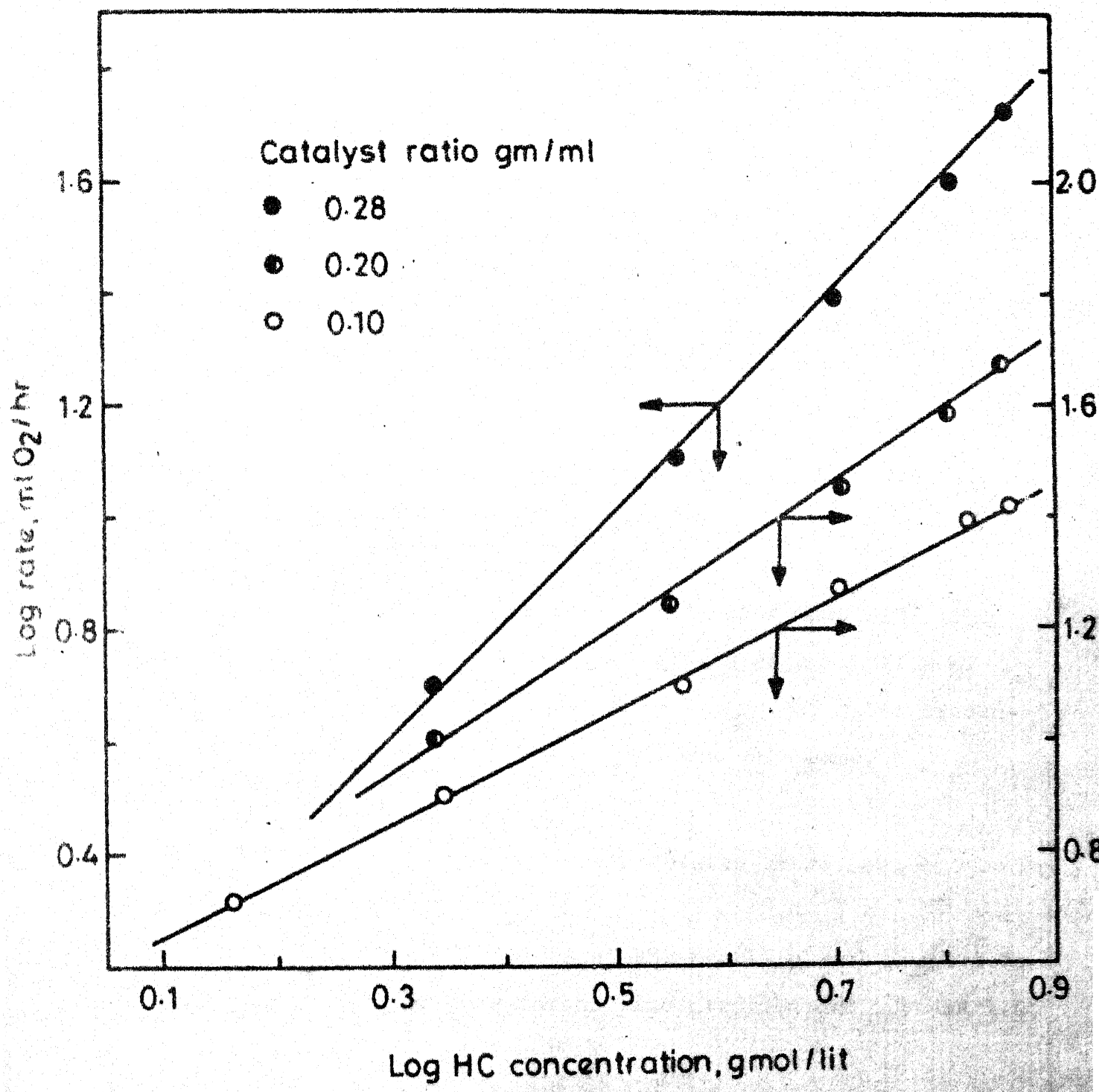

Fig. 4 -The dependence of oxygen absorption rate on tetralin concentration at 65°C.

A log-log plot of rate of oxygen absorption versus catalyst ratio is given in Figure 5. An order of 0.5 was found with respect to the catalyst amount considering all the points at the catalyst ratio below 0.2 gm/ml.

The logarithm of rate of absorption oxygen was plotted with inverse of absolute temperature at the temperatures of 45°, 55°, 65°, 75°, and 85°C. The apparent activation energy for the overall oxidation was calculated to be 11.8 kcal/mole.

4.3.3 Product Distribution

Another important reaction characteristic, that of product distribution, was also obtained from these studies. The products were analysed by Perkin-Elmer Model 137 ir spectrometer. The product distribution as a function of catalyst weight is presented in Table 1. The molar concentration of alcohol and ketone produced were same.

4.3.4 Reaction Mechanism

The experimental results presented above have convincingly shown that:

1. The apparent orders of the reaction with respect to catalyst ratio and hydrocarbon concentration are 0.5 and 1.0 respectively.

2. There is a critical weight of the catalysts above which the rate of oxidation drops sharply and this limiting rate of oxidation is proportional to the square of hydrocarbon

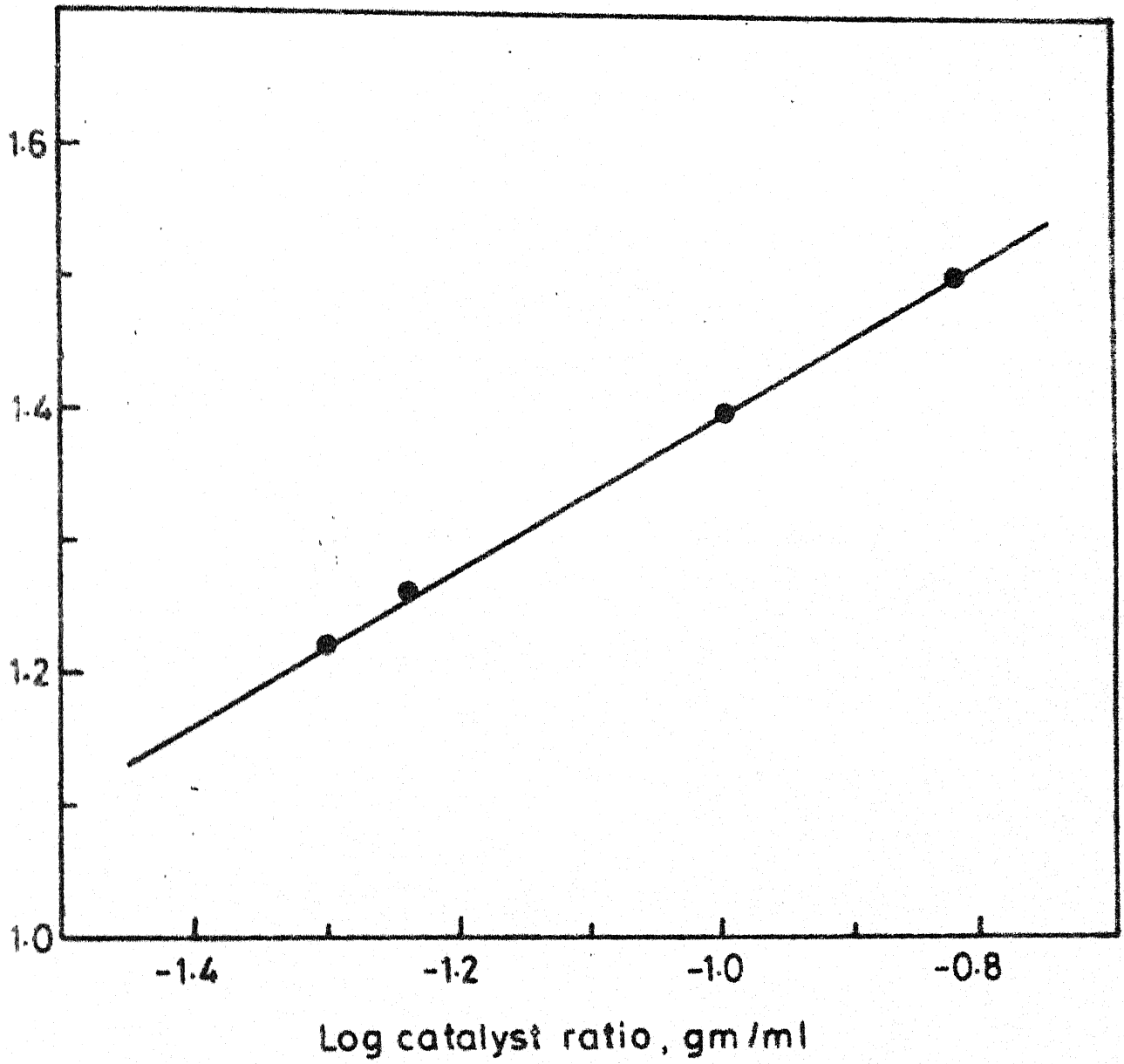

Fig. 5 - The dependence of oxygen absorption rate on the catalyst ratio for tetralin oxidation at 65°C for NiO-20-450-12 catalyst.

TABLE 1: DISTRIBUTION OF PRODUCTS OF TETRALIN OXIDATION

Temperature : 65°C

Duration of Run : 30 minutes

Vol. of Tetralin : 50 ml.

Catalyst weight in gm.	Product Distribution (mole per cent of total oxidized product)		
	Hydroperoxide	Tetralyl Alcohol	Tetralone
1.0	87	7.4	5.6
2.5	80	8.2	11.8
5.0	57.6	21.2	21.2
10.0	44.4	26.0	29.6
15.0	13.3	45.5	41.2

concentration.

To explain the kinetics of cyclohexene oxidation a general mechanism was proposed by Neuberg et al.[7] and used by Srivastava et al. [3,10-11] to explain the kinetics of cumene oxidation. Their scheme is adopted below:

Initiation

$$ROOH + M \underset{}{\overset{k_1}{\rightleftharpoons}} ROOH \ldots\ldots M \qquad (1)$$

$$ROOH \ldots M \underset{}{\overset{k_2}{\rightleftharpoons}} RO^{\cdot} + {}^{\cdot}OH \ldots . M \qquad (2)$$

$$ROOH + {}^{\cdot}OH \ldots M \xrightarrow{k_3} RO_2^{\cdot} + H_2O + M \qquad (3)$$

$$RO^{\cdot} + RH \xrightarrow{k_4} ROH + R^{\cdot} \qquad (4)$$

Propagation

$$R^{\cdot} + O_2 \xrightarrow{k_5} RO_2^{\cdot} \qquad (5)$$

$$RO_2^{\cdot} + RH \xrightarrow{k_6} ROOH + R^{\cdot} \qquad (6)$$

Termination

$$RO_2^{\cdot} + RO_2^{\cdot} \xrightarrow{k_7} \text{inactive products} + O_2 \qquad (7)$$

$$RO_2^{\cdot} + M \underset{}{\overset{k_8}{\rightleftharpoons}} (RO_2^{\cdot} \ldots . M) \qquad (8)$$

$$RO_2^{\cdot} + (RO_2^{\cdot} \ldots . M) \xrightarrow{k_9} \text{inactive products} \qquad (9)$$

If the termination rate of peroxy radicals on the catalyst surface (Eqs. 8 and 9) is negligible compared with the biradical termination rate (Eq.7) then the rate of oxidation will be given by

$$\frac{-d[O_2]}{dt} = K_6 \left(\frac{R_i}{2K_7}\right)^{1/2} [RH]$$

It may be assumed that R_i is proportional to amount of catalyst. The experimental orders agree well with the derived rate expression.

If it is assumed that at the limiting rate of oxidation of rate of formation of hydroperoxide through reaction (6) becomes equal to the rate of decomposition then the limiting rate of oxidation is given as

$$\frac{-d[O_2]}{dt} = \frac{\alpha K_6^2 [RH]^2}{2K_7 + K_8 K_9 [M]}$$

where α is the fraction of hydroperoxide yielding free radicals. The derivation is similar to one proposed by Neuberg et al.[7]. The reaction order of this expression is consistent with the experimental results of the present work. Therefore, it can be concluded that the catalytic activity of supported NiO is mainly due to the capability of decomposing hydroperoxide in the chain initiating radicals. The similarity in the kinetic behaviour of cyclohexene and tetralin may be due to formation of resonance stabilized radical species ($R^{\cdot}$) in each of these cases.

4.4 CONCLUSIONS

The catalyst having 20 per cent by weight of NiO on Al_2O_3 heat treated at 450°C for 12 hours showed the maximum rate. An order of one was found with respect to hydrocarbon concentration in the region where the limiting rate of oxidation was not attained while an order of 2 was found in the region where the limiting oxidation is reached. An order of 0.5 was found with respect to catalyst amount. The apparent activation energy for the overall oxidation was 11.8 Kcal $mole^{-1}$. A mechanism was proposed to fit the data. The kinetic expression derived was well in line with the experimental rate equation.

The catalytic activity of supported NiO is mainly due to the capability of decomposing hydroperoxide in the chain initiating radicals.

REFERENCES

1. George, P., Trans. Faraday. Soc. 42, 210 (1946).
2. Mukherjee, A., and Graydon, W.F., J. Phy. Chem. 71, 4232(1967)
3. Agarwal, A.K., and Srivastava, R.D., J. Catal. 39, 317 (1975).
4. Neuburg, H.J., Basselt, J.M., and Graydon, W.F., J. Catal. 25, 425 (1972).
5. Verma, G.R., and Graydon, W.F., J. Catal. 28, 236 (1973).
6. Srivastava, R.K., and Srivastava, R.D., J.Catal. 39, 317(1975)
7. Neuburg, H.J., Phillips, M.J., and Graydon, W.F., J. Catal. 38, 33 (1975).
8. George, P., and Robertson, A., Trans. Faraday Soc. 42, 227 (1946).
9. Arthur, E.W., and Robert, B.M., J. Am. Chem. Soc. 75, 6189 (1953).
10. Krishna, L.V.G., Rao, M.S., and Srivastava, R.D., J. Catal. 49, 109 (1977).
11. Krishna, L.V.G., Srivastava, R.D., and Rao, M.S., J. Appl. Chem. Biotech. 27, 522 (1977).
12. Prasad, M., and Tendulkar, M.G., J.Chem.Soc. 1403 (1931).
13. LeBlanc, V.M., and Sachse, H.N., Z. Elektrochem. 32, 204 (1926
14. Tourkey, A.R., Hanafi, Z., Salem, T.M., Z. Phy. Chem. (Leipzic 243, 145 (1970).
15. Dollimore, D., and Jones, E., J. Appl. Chem. Biotech. 23, 29 (1973).